Electron Energy Loss Spectroscopy

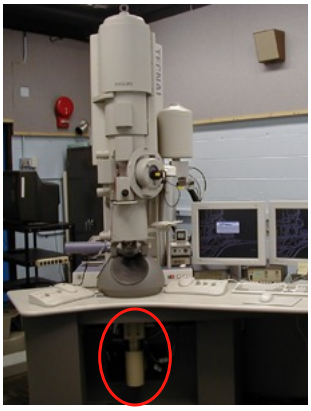

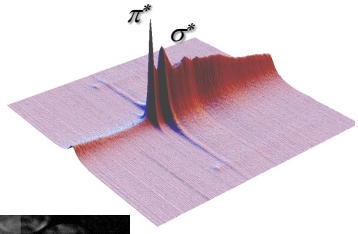

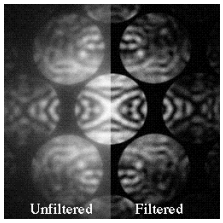

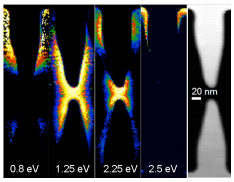

1

The Energy Loss Processes

Instrumentation: Detector Systems

Instrumentation: AEM Systems

Data Analysis and Quantification:

Advanced Topics

2

Electron Energy Loss Spectroscopy

- Measure the changes in the inelastic scattering distribution of an electron beam transmitted through a thin specimen.
- Each type of interaction between the electron beam and the specimen produces a characteristic change in the energy and angular distribution of scattered electrons.
- The energy loss process is the primary interaction event. All other sources of analytical information (i.e. X-rays, Auger electrons, etc.) are secondary products of the initial inelastic event. Thus, EELS has the highest potential yield of information/inelastic event

3

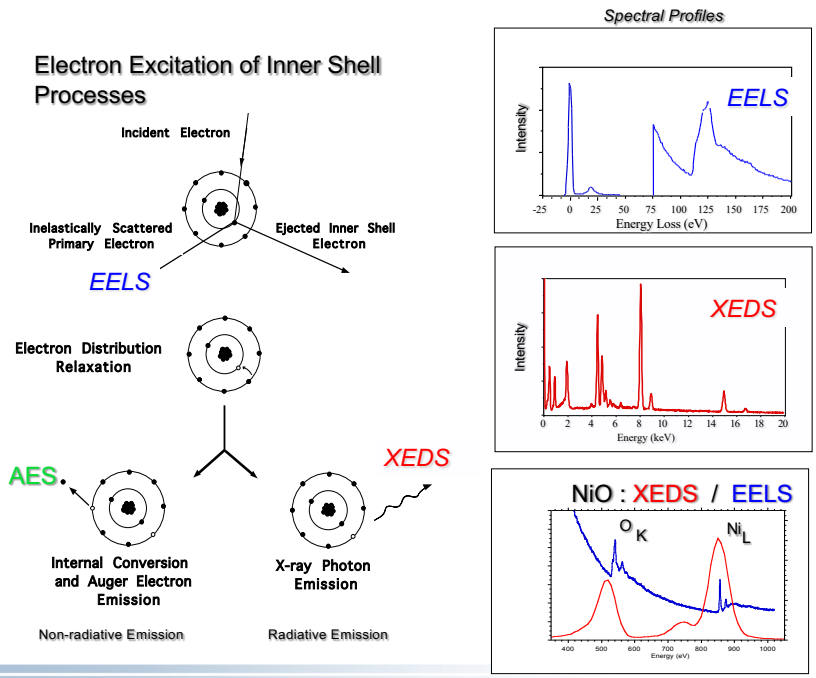

4

Electron Energy Loss Spectroscopy

- Measure the changes in the inelastic scattering distribution of an electron beam transmitted through a thin specimen.
- Each type of interaction between the electron beam and the specimen produces a characteristic change in the energy and angular distribution of scattered electrons.
- The energy loss process is the primary interaction event. All other sources of analytical information (i.e. X-rays, Auger electrons, etc.) are secondary products of the initial inelastic event. Thus, EELS has the highest potential yield of information/inelastic event

5

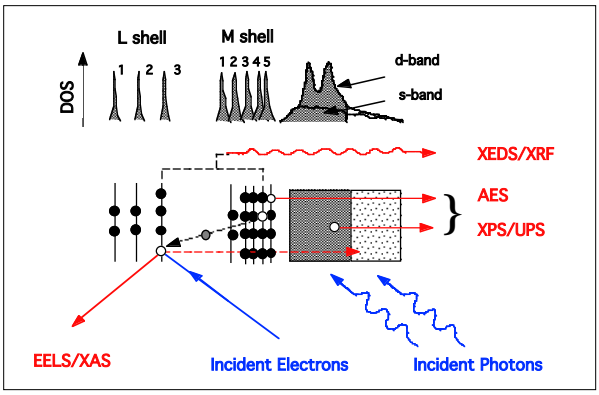

Schematic Diagram Illustrating Sources of Inelastic Scattering Signals

6

Experimental XEDS, XPS, and EELS data from the Copper L shell. Note the differences in energy resolution, and spectral features.

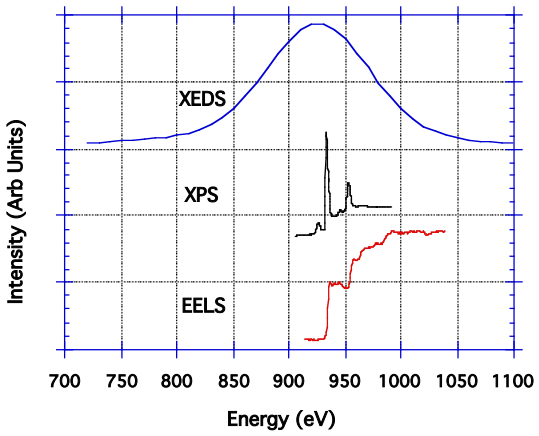

7

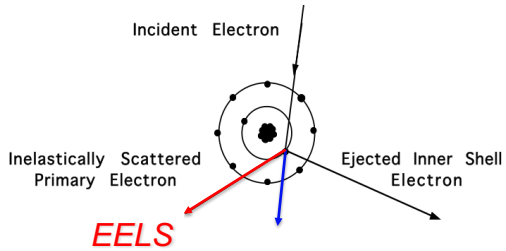

The Energy Spectral Profile

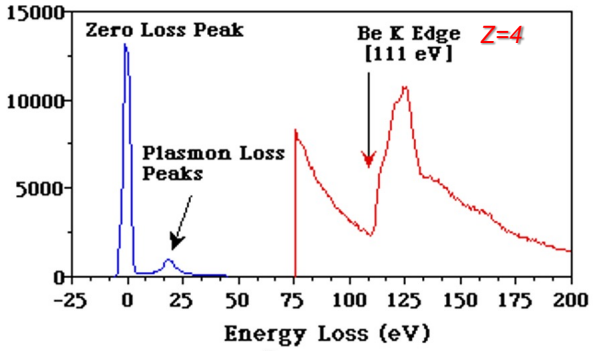

8

Plasmon Energies of some Elements

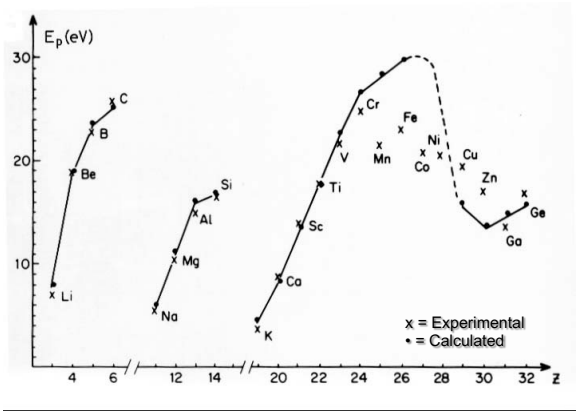

$E_p = (h/2\pi)(ne^2/\varepsilon_0 m)^{1/2} = (28.8eV)\,(z\rho/A)^{1/2}$

n = density of "outer-shell" electrons,
z = valency (free-e/atom)

Colliex 1984

9

Table 1. Edges Suitable for EELS Microanalysis for the Energy Range 0-3 keV

Atomic Number	Inner Shell	Spectroscopic Notation
Z = 1-11	K	1s
Z = 12-17	K L_3,L_2,L_1	1s $2p_{3/2},2p_{1/2}$,2s
Z = 19-45	L_3,L_2,L_1 M_{54},M_{32},M_1	$2p_{3/2}$,.--> $3d_{5/2},3d_{3/2}$, $3d_{1/2}$, $3p_{3/2},3p_{1/2}$,3s
Z = 46-79	M_{54},M_{32},M_1 N_{45},N_{32},N_1 O_{32},O_1	$3d_{5/2}$,..--> $4d_{5/2},4d_{3/2},4d_{1/2}$, $4p_{3/2},4p_{1/2}$,4s $5p_{3/2},5p_{1/2}$,5s
Z > 80	N_{67},N_{45},N_{32},N_1 O_{45},O_{32},O_1	$4f_{7/2}$,.--> $5p_{3/2}$.-->

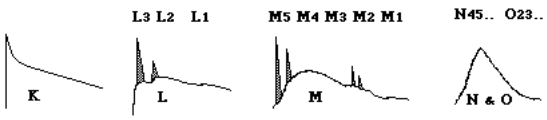

Figure 5. Schematic illustration of K, L, M, N and O Edge shapes, the "white lines" sometimes detected on L and M shells are shown shaded peaks at the edge onsets. In all sketches the background shape has been omitted for clarity. These profiles should be compared with experimental profiles of figure 6.

10

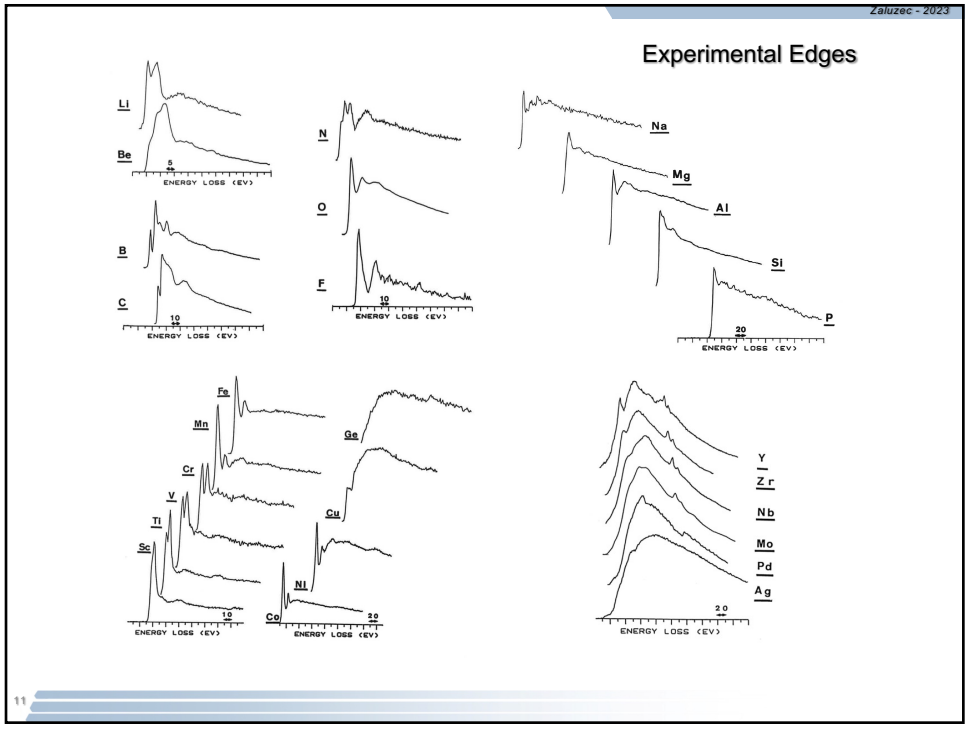
Zaluzec - 2023
Experimental Edges
Li
Be
B
C
N
O
F
Na
Mg
Al
Si
P
Fe
Mn
Cr
V
Ti
Sc
Ge
Cu
Ni
Co
Y
Zr
Nb
Mo
Pd
Ag
ENERGY LOSS (EV)
11

11

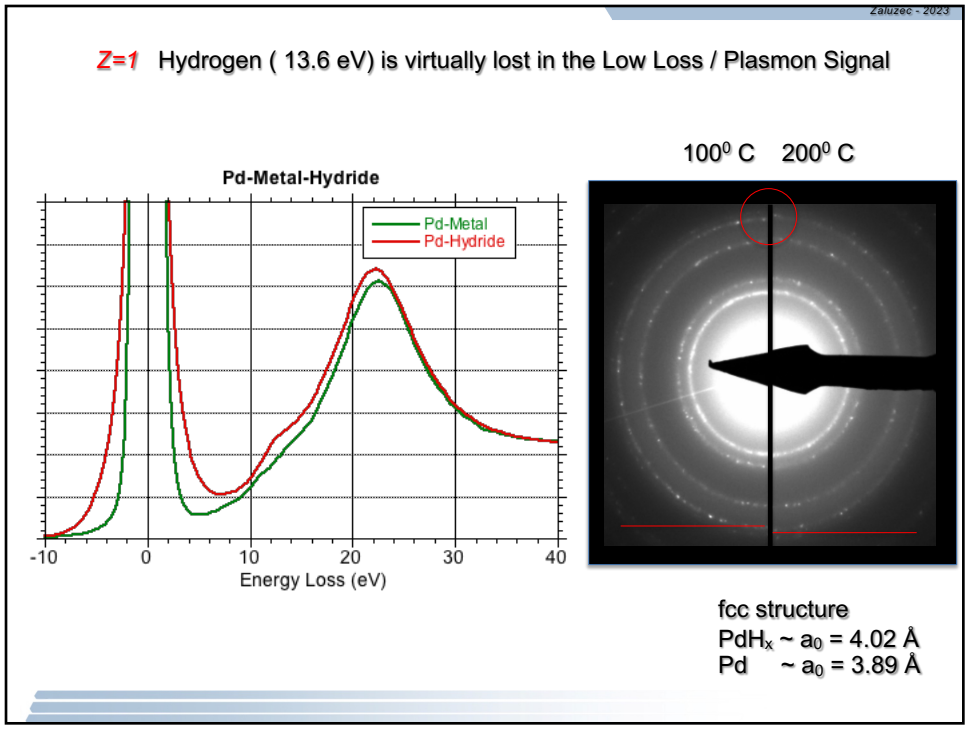
Zaluzec - 2023
Z=1 Hydrogen (13.6 eV) is virtually lost in the Low Loss / Plasmon Signal
Pd-Metal-Hydride
Pd-Metal
Pd-Hydride
-10
0
10
20
30
40
Energy Loss (eV)
100⁰ C 200⁰ C
fcc structure
PdHx ~ a0 = 4.02 Å
Pd ~ a0 = 3.89 Å

12

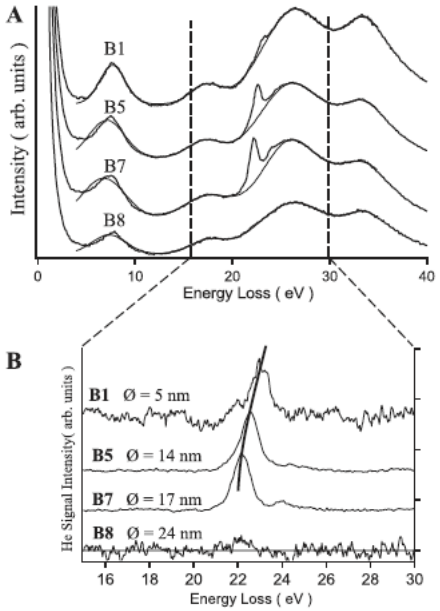

Helium
In Pd

Z=2

D. Taverna etal
PRL 100, 035301 (2008)

13

Electron Energy Loss Spectroscopy of Lithium Compounds

Conventional Core Loss Spectroscopy
Generally Requires ~ 1-2 eV Resolution

LiF Spectroscopy

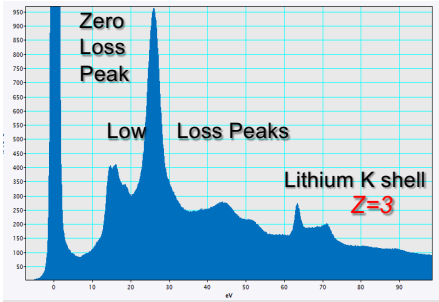

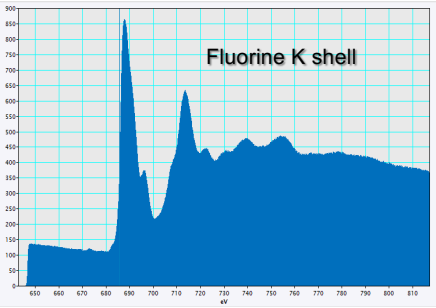

14

Electron Scattering

Elastic Scattering

Single Atoms:

$$I(\theta) \sim |f(\theta)|^2 = |f_o|^2 \bullet \frac{1}{(\theta^2 + \theta_o^2)^2}$$

$$\theta_o = \frac{1}{2\pi(0.885 a_o Z^{-1/3})}$$

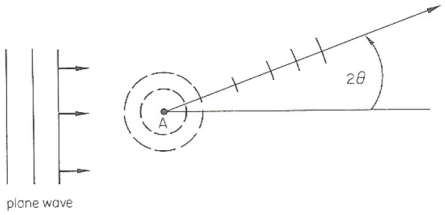

Figure 2.2 The scattering of a plane wave at an atom A through the formation of spherical wavelets travelling at an angle 2θ to the original direction of motion

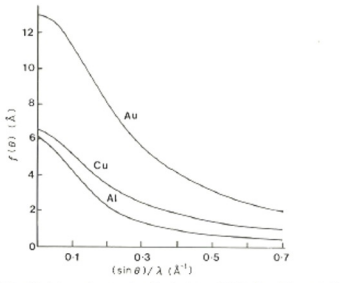

Fig. 2.2 Relationship between the atomic scattering factor $f(\theta)$ (in Å) and the scattering angle $(\sin\theta)/\lambda$ (in Å^{-1}) for aluminium, copper and gold calculated using equation (2.1).

Scattering from an isolated atom in free space

15

15

Scattering from an collection of an amorphous collection of atoms
- neighboring atoms give rise to interference

Amorphous Solids:

$$I(\theta) \sim |f(\theta)|^2 \bullet \left\{1 + \frac{\sin(kR)}{kR}\right\}$$

$$k = \frac{4\pi}{\lambda}\sin(\theta)$$

R = Average Interatomic Spacing

Amorphous Silica (SiO_2)

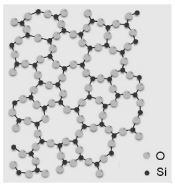

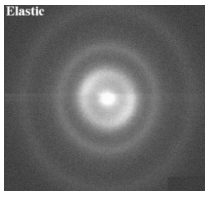

16

16

Phonons:

$$I(\theta) \sim |f(\theta)|^2 \bullet \{1 - e^{-2M}\}$$

$$M = \frac{8\pi \langle u^2 \rangle \sin(\theta)}{\lambda}$$

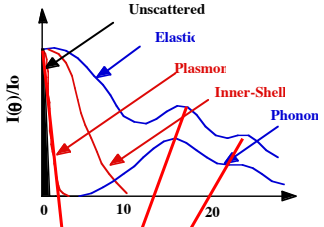

Inelastic:

$$I(\theta) = \Gamma(\delta E, \theta) \bullet \frac{1}{\theta^2 + \theta_E^2}$$

$$\theta_E = \frac{\Delta E}{2\gamma_0 T_0} \qquad \gamma_0 = \frac{1}{\sqrt{1-\beta^2}}$$

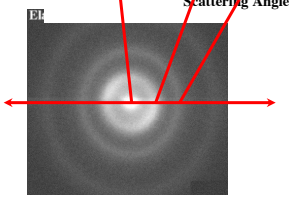

$\Gamma(\delta E,\theta)$: Imaginary Part of the Complex Dielectric constant(ε)
: Generalized Oscillator Strength

17

17

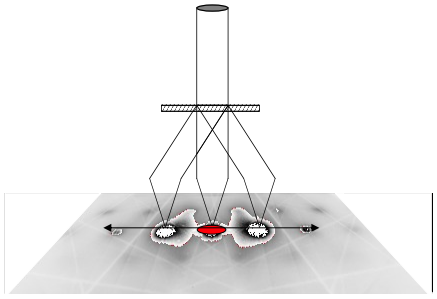

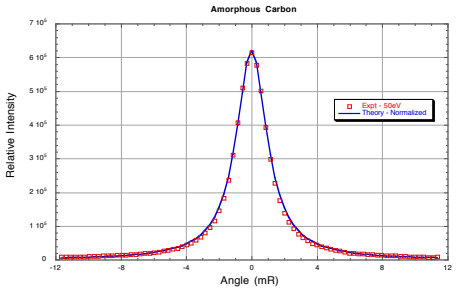

Inelastic:

$$I(\theta) = \Gamma(\delta E, \theta) \bullet \frac{1}{\theta^2 + \theta_E^2}$$

$$\theta_E = \frac{\Delta E}{2\gamma_0 T_0} \qquad \gamma_0 = \frac{1}{\sqrt{1-\beta^2}}$$

$\Gamma(\delta E,\theta)$: Imaginary Part of the Complex Dielectric constant(ε)
: Generalized Oscillator Strength

18

18

Typical Scattering Angles

$$\theta_E = \frac{\Delta E}{2T_0}$$

$$T_0 = \gamma m_0 c^2$$

$$\theta_B = \arcsin\left(\frac{\lambda}{2d}\right) \approx \frac{\lambda}{2d}$$

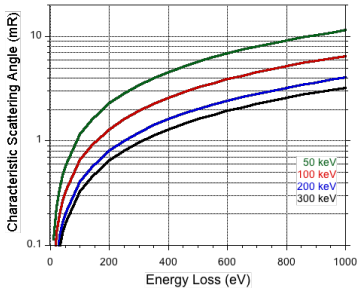

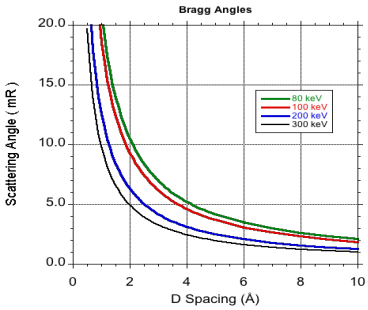

d D-spacing
λ Electron Wavelength
θ_E Characteristic/Mean Scattering angle
ΔE Energy Loss
T_o Electron Kinetic Energy

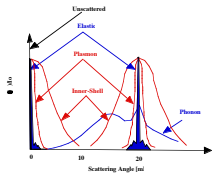

19

Intensity of Edges is Directly Related to Mean Scattering Angle
Example: Amorphous Carbon (Z=6)

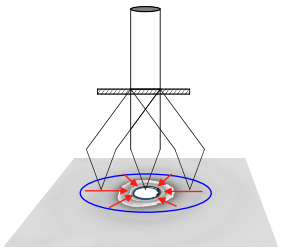

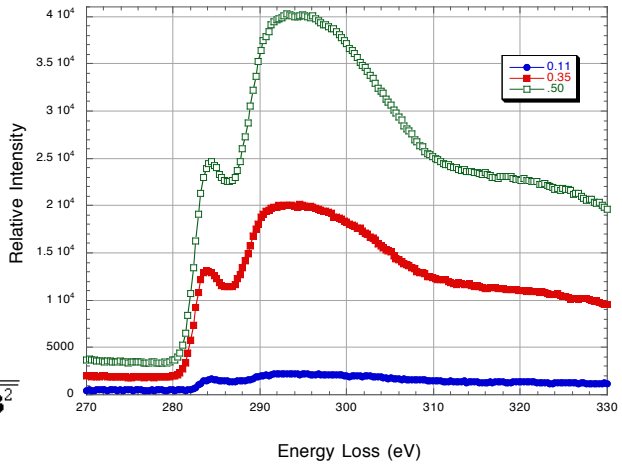

$$\theta_E = \frac{\Delta E}{2\gamma_0 T_0} \qquad \gamma_0 = \frac{1}{\sqrt{1-\beta^2}}$$

θ_E~1.15 mR

20

20

Intensity of Edges is Directly Related to Mean Scattering Angle
Example: Boron – Nitride

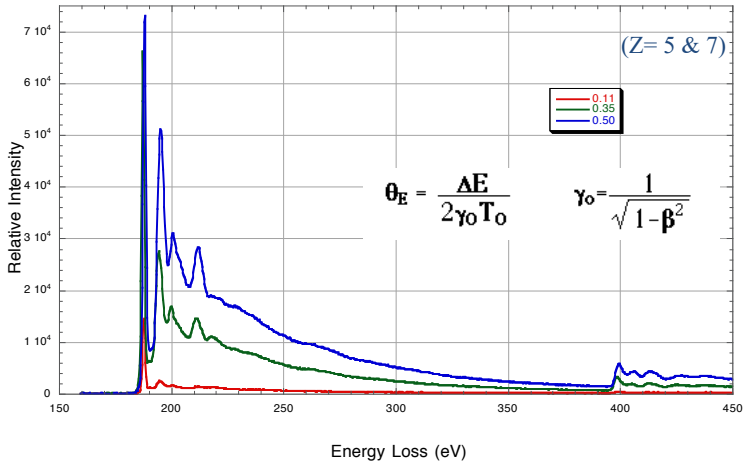

θ_E ~0.777 mR θ_E ~1.62 mR

21

21

Type of Electron Scattering	Angular Range	Energy Loss
Unscattered	0	0
Elastic	10's-100's mR	~0
Phonon	10's-100's mR	<.025 eV
Inelastic	10's mR	everything else
Plasmon	< 1mr	10's of eV
Inner-Shell	~10's of mR	10's-1000's eV

Elastic Scattering

Crystalline Solids:

$$I(\theta) \sim |F(hkl)|^2$$

$$F(hkl) = \sum_j f_j(\theta)\ e^{(-2\pi i \vec{k}\cdot\vec{r})}$$

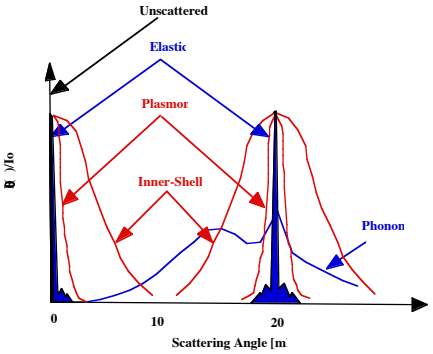

Elastic Scattering Introduces additional angular dependence via Diffraction

22

Plasmon Dispersion Surfaces

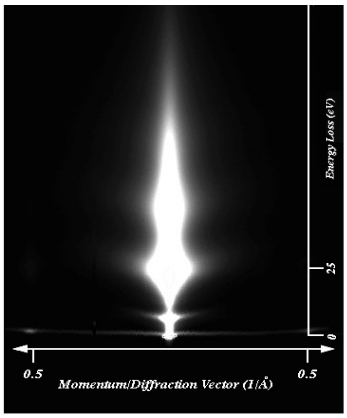

Graphite

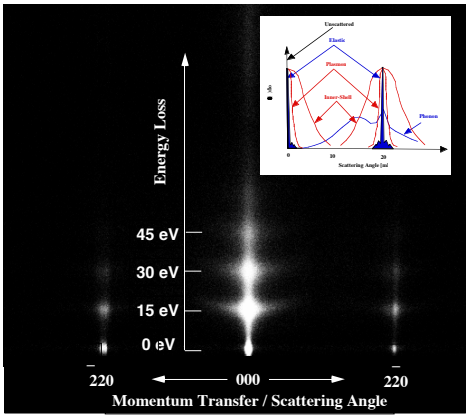

Silicon

23

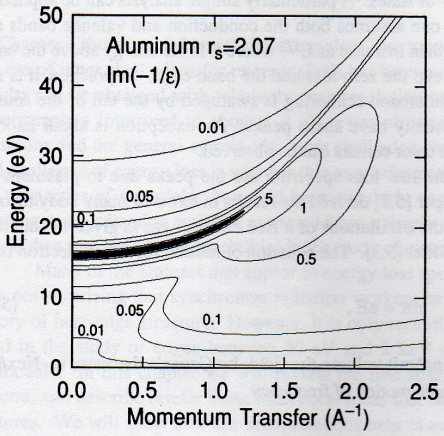

Figure 5-1. Im[-1/ε(q,ω)] for aluminium showing the volume plasmon and its dispersion (change in energy as a function of momentum transfer, q) (Courtesy of P. E. Batson).

24

Zaluzec - 2023

Inelastic:

$$I(\theta) = \Gamma(\delta E,\theta) \bullet \frac{1}{\theta^2 + \theta_E^2}$$

$$\theta_E = \frac{\Delta E}{2\gamma_0 T_0} \qquad \gamma_0 = \frac{1}{\sqrt{1-\beta^2}}$$

$\Gamma(\delta E,\theta)$: Imaginary Part of the Complex Dielectric constant(ε)
: Generalized Oscillator Strength

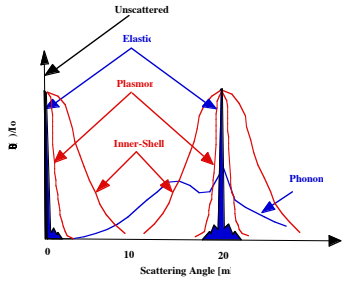

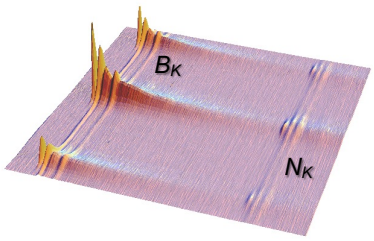

Elastic Scattering Introduces additional angular dependence via Diffraction

25

Zaluzec - 2023

Core Loss Dispersion Surface

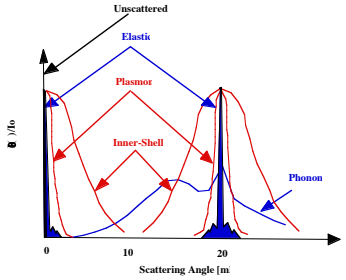

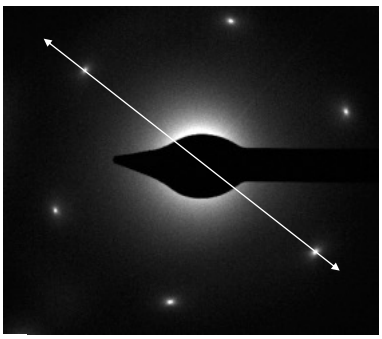

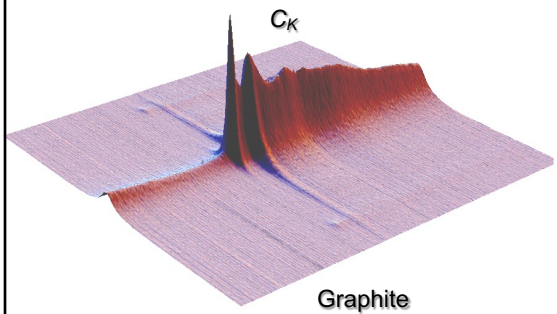

Graphite

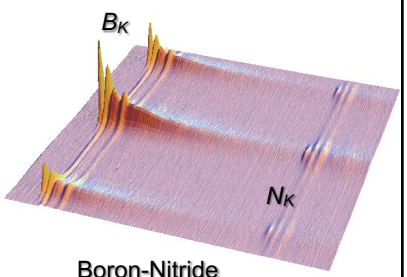

Boron-Nitride

26

Instrumentation: Detector Systems

Energy Loss Spectrometers
- Basic Principles
- Electrostatic/Electromagnetic
- Serial/Parallel Detector Systems
- Spectral Artifacts

Multichannel Analyzers

27

Force (F) and displacements (X) on electrons by different types of fields yields a deflection in their trajectory. In a uniform field region the electrons drift at a characteristic radius (R).

Electrostatic

$$\vec{F}_E = q\,\vec{E} \qquad X_E = \frac{1}{2}\frac{qEL^2}{m_o v^2} \qquad R_E = \frac{m_o v^2}{qE}$$

Electromagnetic

$$\vec{F}_B = q\left[\vec{v}\times\vec{B}\right] \qquad X_B = \frac{1}{2}\frac{qBL^2}{m_o v} \qquad R_B = \frac{m_o v}{qB}$$

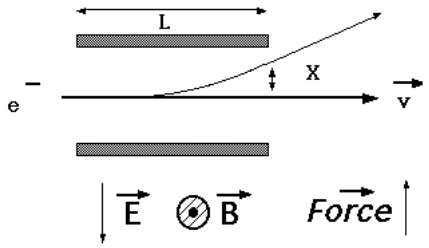

28

Basic Spectrometer

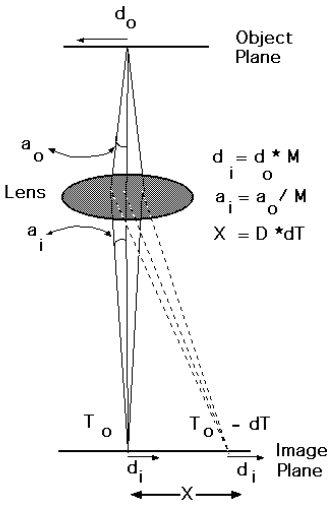

Types of Electron Spectrometers:

Electrostatic:	**Mollenstedt**
Electrostatic/magnetic:	**Wien, Castaing-Henry**
Electromagnetic:	**Cylindrical, Omega, Sector**

29

29

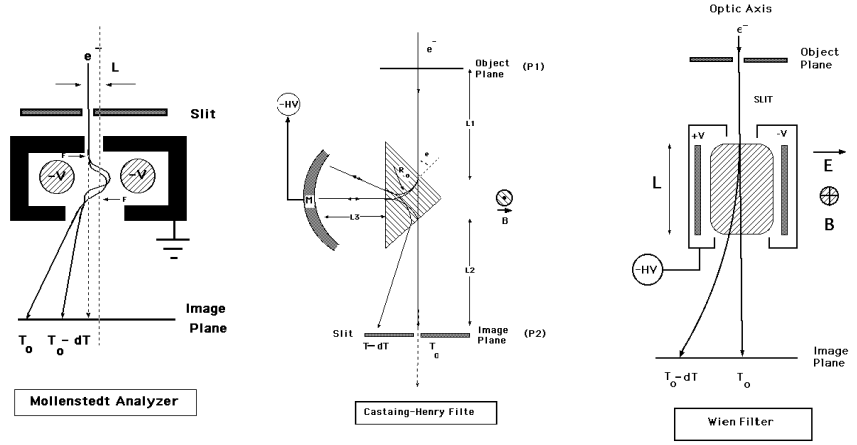

30

30

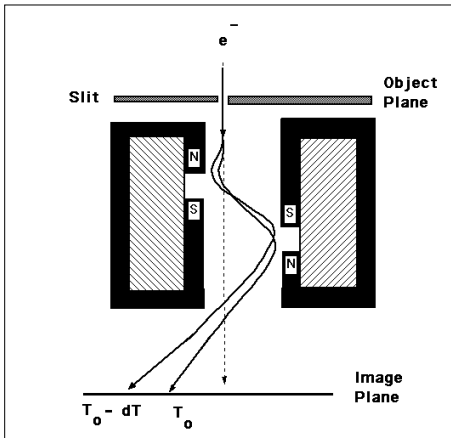

Cylindrical Magnetic Analyzer

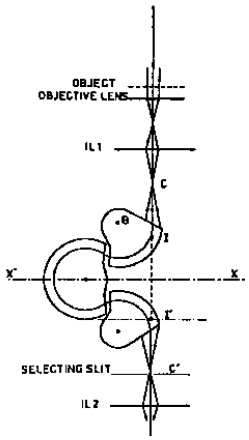

Omega Filter

31

Magnet Sector Analyzer

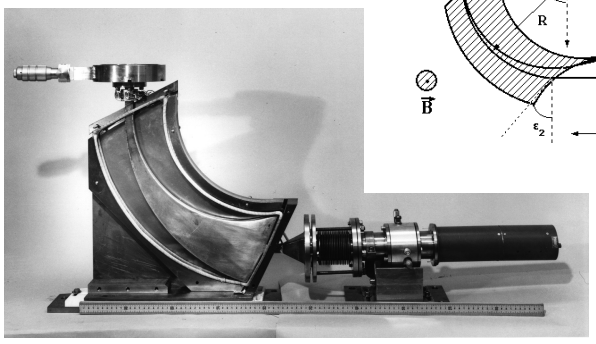

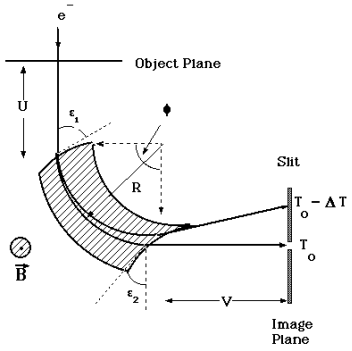

32

Zaluzec - 2023

Data Collection Parallel Detectors

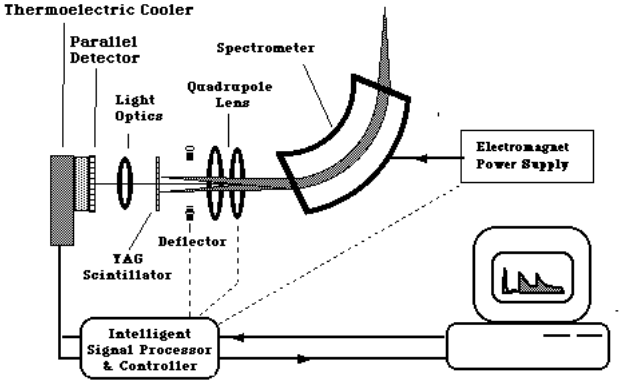

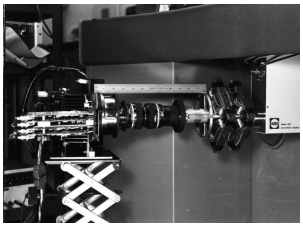

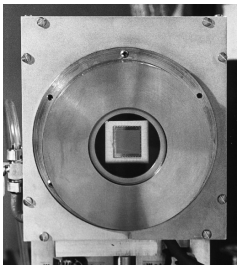

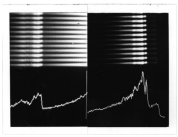

Major Components

Spectrometer
Computer
Magnet Power Supply
Quadrupole Lenses, Deflectors, & Power Supplies
Scintillator, Parallel Detector, Thermoelectric Cooler
Intelligent Signal Processor

33

Zaluzec - 2023

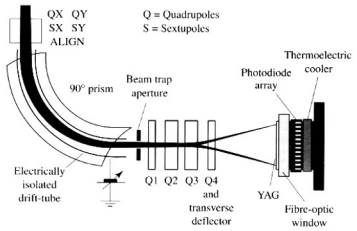

Figure 3.3. Schematic diagram of a Gatan PEELS system. Redrawn from Egerton (1996) *Electron Energy Loss Spectroscopy in the Electron Microscope*, 2nd Edn, with permission of Plenum Publishers.

Commerical Spectrometers Vs Imaging Filters

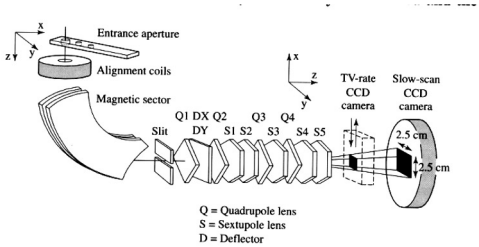

Figure 3.4. Schematic diagram of a Gatan imaging filter. Redrawn from Egerton (1996) *Electron Energy Loss Spectroscopy in the Electron Microscope*, 2nd Edn, with permission of Plenum Publishers.

34

34

Spectral Imaging
Slice-by-Slice vs Point-by-Point

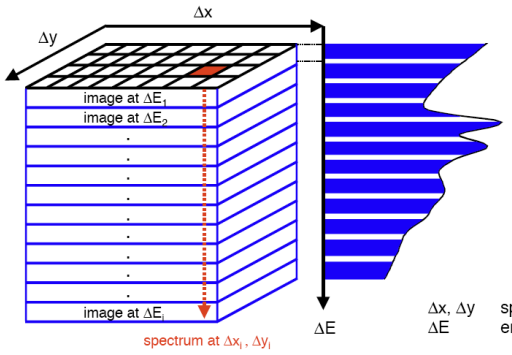

The technique of building up a more or less complete data cube is termed **Spectrum Imaging**

Δx, Δy spatial dimensions
ΔE energy-loss dimension

EFTEM Spectrum Imaging:
- Energy filtered broad beam technique
- fills data cube one image plane at a time
- less time

STEM Spectrum Imaging:
- Focused probe method
- fills data cube one spectrum at a time
- less dose

35

Energy Filtering in Thick Specimens

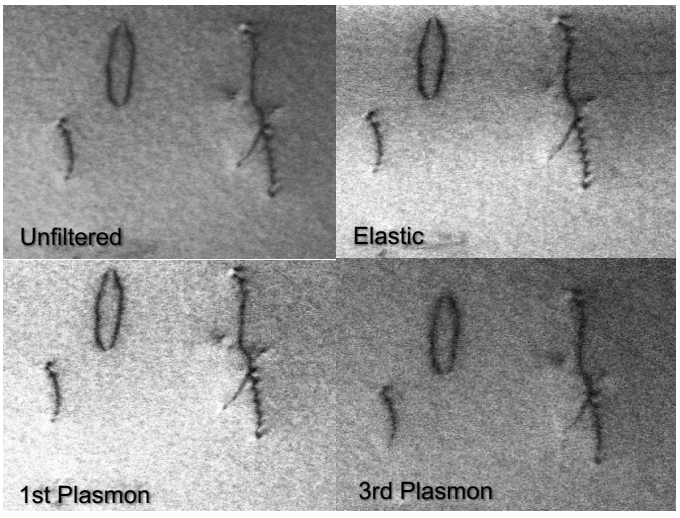

36

Silicon 111 ZAP- Gamma Corrected

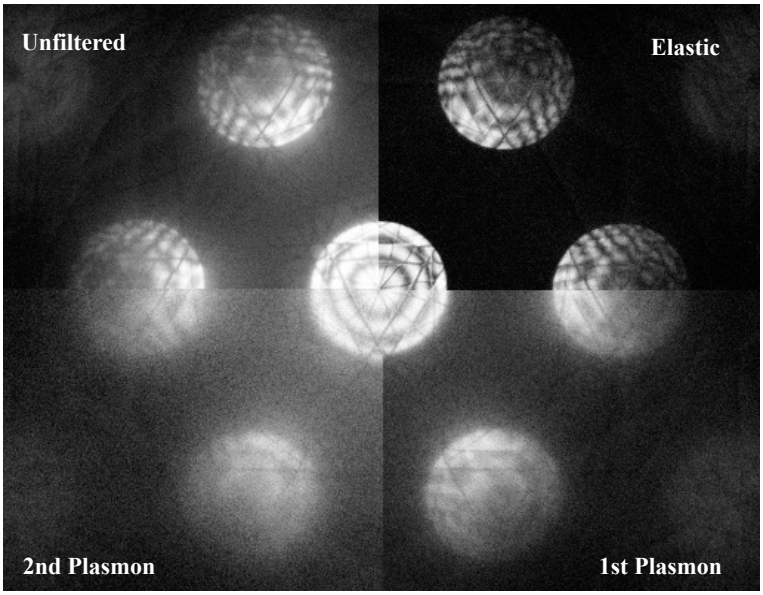

37

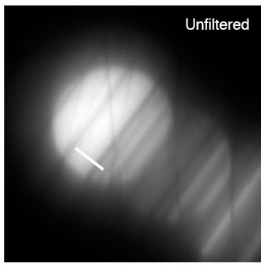

Silicon [110]

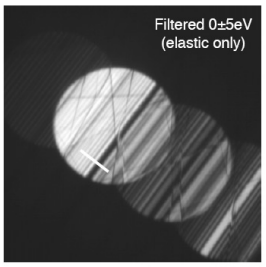

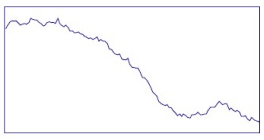

essential for
quantitative CBED

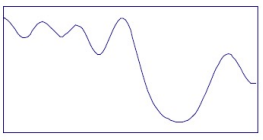

38

Spectroscopy vs Filtered Imaging

Information without EFTEM

Information gain with EELS + EFTEM

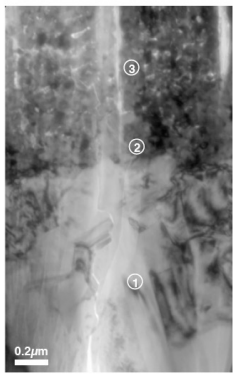

Unfiltered bright field image - structural contrast only

Interface Titanium alloy and PVD-grown Gadoliniumboride

EELS spectra

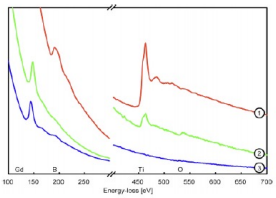

from conventional TEM images
via EEL-spectra
to energy-filtered images
showing elemental distributions

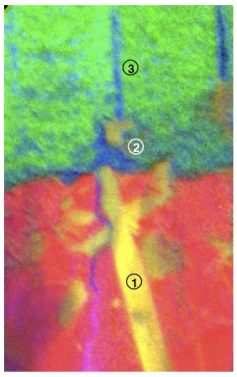

Titanium Boron Oxygen

EFTEM - Elemental contrast

39

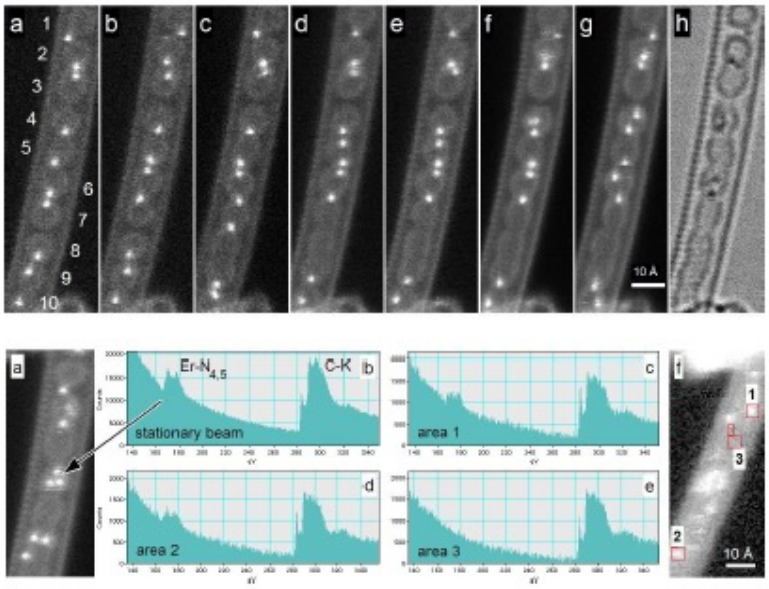

Krivanek etal 2010

40

What is the Goal of the EELS Experiment

- Detection
- Quantification
- Filtering (Elastic vs Inelastic Signal)
- Spatial Distribution (HyperSpectral Imaging)
- High Resolution Spectroscopy …

41

Data Analysis and Quantification:

Spectral Processing
Thin Film Quantification Methods
Specimen Thickness Effects

42

42

Measurement of Parameters required for EELS Quantification

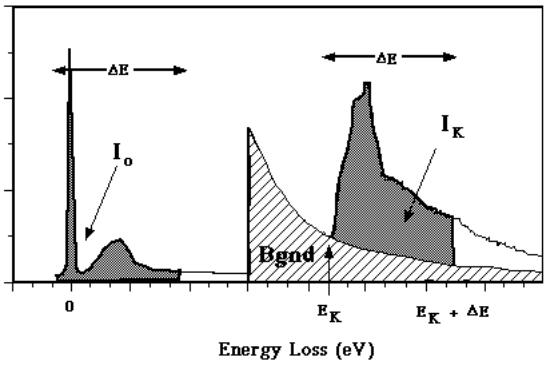

43

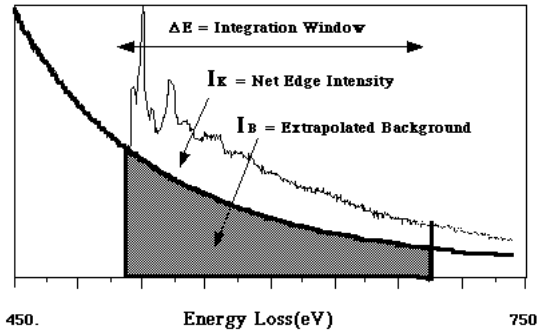

44

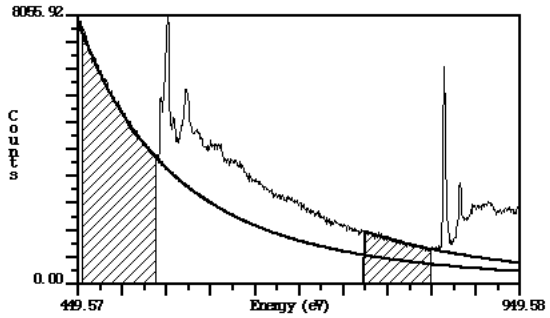

Most Frequently Used Model in the Medium Loss Regime

$$I_{Bgnd} = A\ E^{-R}$$

$2 \leq R \leq 7$ typical values for 200 eV < E < 1500 eV

Other Background Models Used are Phenomenological

N^{th} Order Polynominal & Log-Polynominal mainly used < 200 eV Loss

45

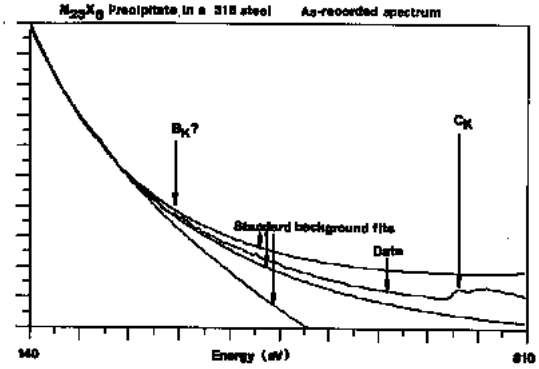

Conventional Background Fitting does not always allow the user to find small peaks in high background areas.

46

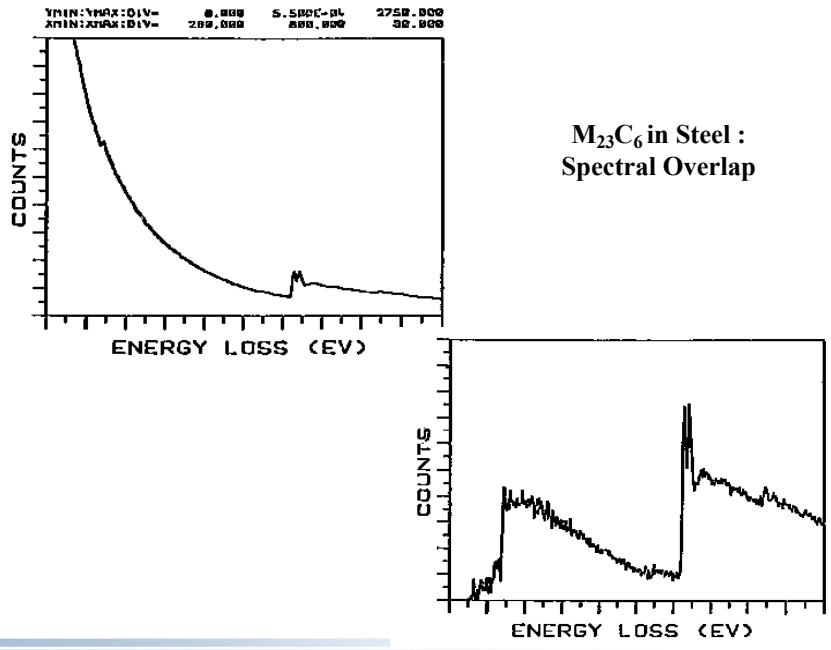

$M_{23}C_6$ in Steel : Spectral Overlap

47

47

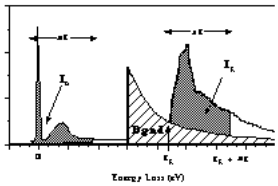

$$I_k = P_k * I_o$$

I_k = Number of electron having excited a kth inner shell

P_k = Probability of excitation of the kth shell

I_o = Incident electron current

$$P_k = N \sigma_k$$

N = Number of atoms of the element analyzed
σ_k = Ionization cross-section for the kth shell

$$N = \frac{I_k}{\sigma_k \; I_o}$$

48

48

Alternatively;

Consider the ratio of Intensities of any two Edges in the same spectrum I_A and I_B

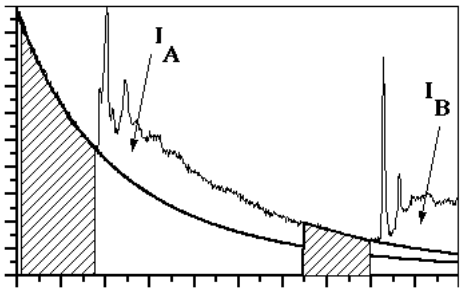

Invoke the Ratio Method and obtain the exact equation:

$$\frac{I_A}{I_B} = \frac{\sigma_A}{\sigma_B}\frac{N_A}{N_B}$$

Note the similiarity of this equation with that of Thin Film XEDS

49

49

But in the real world the assumptions used in the above simple arguments are never realized:

- Measure all scattered electrons ($\beta=\pi=180^0$)
- Integration over all energy Losses

Because we must measure over a finite energy window (δE) we modify the expression to:

$$N_A = \frac{I_A(\delta E)}{\sigma_A(\delta E)*I_0}$$

we also measure over a finite angular window (β) and therefore, we modify the expression to:

$$N_A = \frac{I_A(\delta E,\beta)}{\sigma_A(\delta E,\beta)*I_0}$$

and the ratio equation becomes:

$$\frac{N_A}{N_B} = k_{AB}\frac{I_A(\delta E,\beta)}{I_B(\delta E,\beta)}$$

with

$$k_{AB} = \frac{\sigma_B(\delta E,\beta)}{\sigma_A(\delta E,\beta)}$$

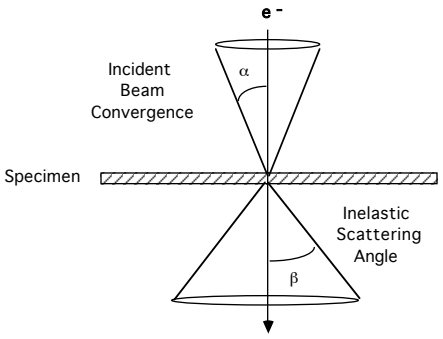

50

50

By measuring $\mathcal{N}$ edges we have $\mathcal{N}$-1 equations, if we invoke the argument that the compositions must sum to unity

$$\sum_{i=1}^{\mathcal{N}} C_i = 1$$

we arrive at a set of $\mathcal{N}$ equations and $\mathcal{N}$ unknowns which can be solved by simple algebra.

For example:

- if $N_A/N_B = 2.$; then $N_A = 2\ N_B$
- if $N_A + N_B = 1$; then $3N_B = 1$ or $N_B = 0.33$
- and $N_A = 1 - N_B = 0.67$

51

51

Measuring Incident and Scattering Solid Angles

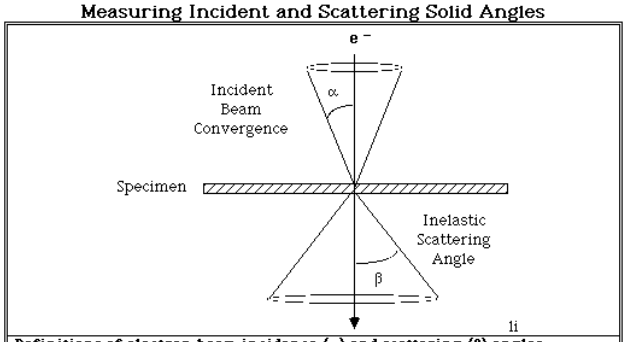

Definitions of electron beam incidence (α) and scattering (β) angles

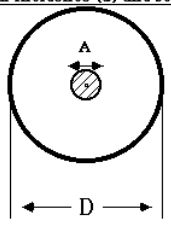

Figure 1.4 Measurement of convergence or scattering angles by comparison to a polycrystalline diffraction pattern of a standard.

$$\alpha \text{ or } \beta = \frac{A}{D} * 2\ \text{Arcsin}\left(\frac{\lambda}{2d}\right) \qquad \lambda = \frac{12.27}{\sqrt{V_o(1+0.978x\ 10^{-6}V_o)}}$$

52

52

Hexagonal Boron- Nitride

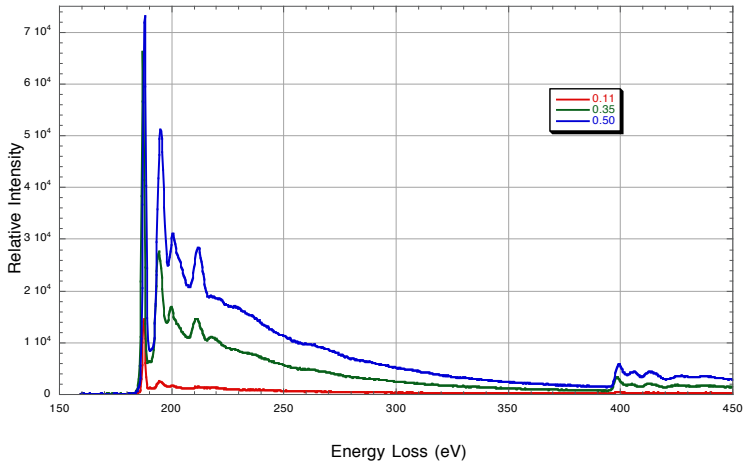

θ_E ~0.777 mR θ_E ~1.62 mR

53

Problems in EELS Quantification
Cross-section Calculations

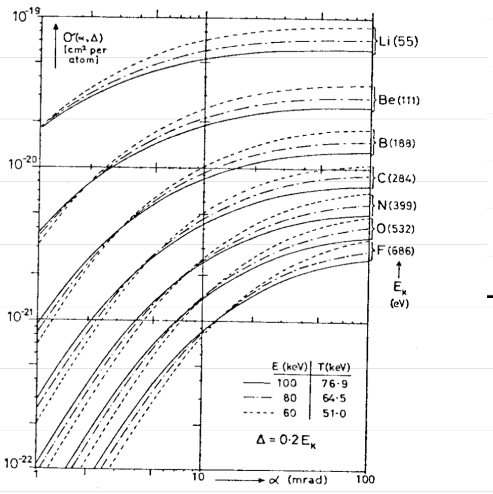

Fig. 3. K-shell partial cross-sections for first-row elements with $\Delta = 0.2\,E_K$ and incident electron energies of 60, 80 and 100 keV.

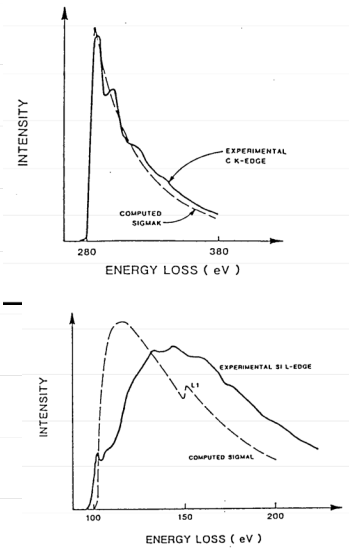

Figure 5 Comparison of an experimental L edge profile with the equivalent profile calculated by using the SIGMAL model.

54

Problems In EELS Quantification
Collection Angle Issues

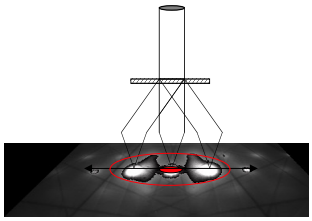

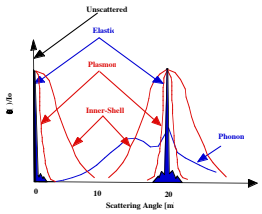

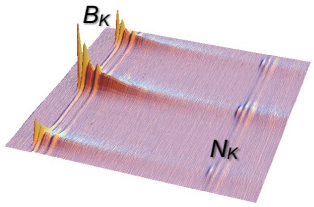

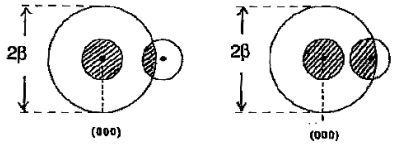

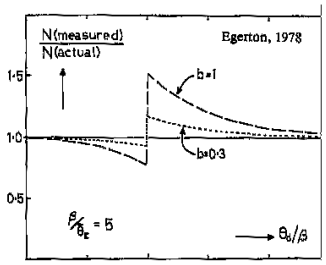

55

55

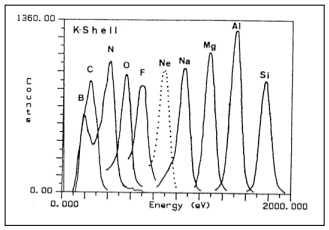

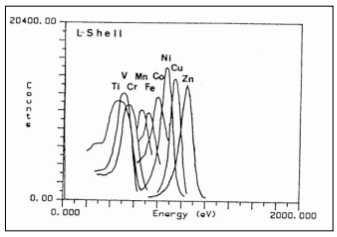

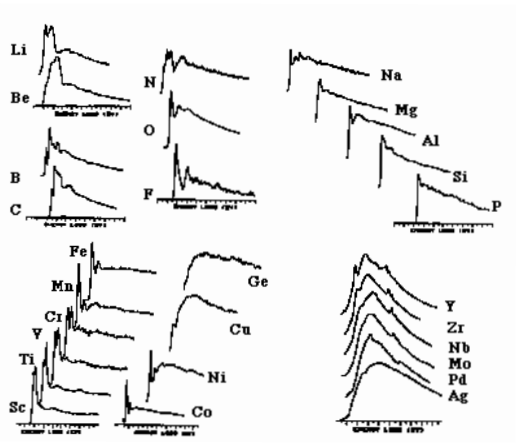

Zaluzec - early 1980s

56

316 SS - ppt
TiN- $M_{23}C_6$

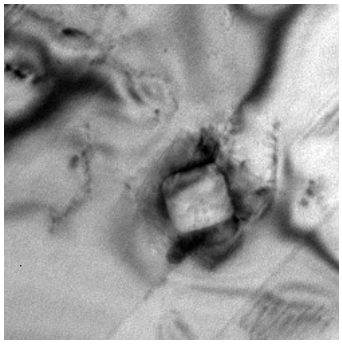

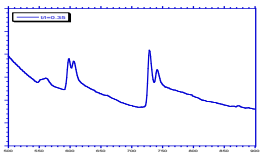

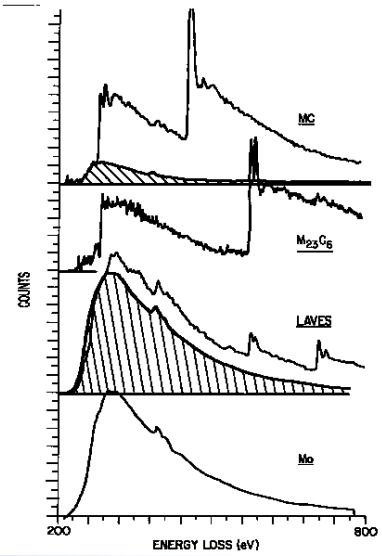

57

316 SS - ppt
TiN- $M_{23}C_6$

EELS/EFTEM Map

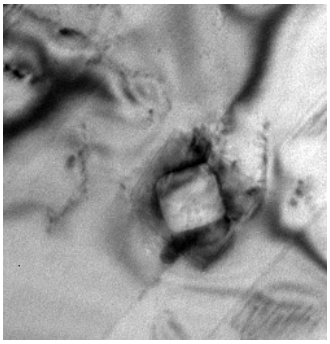

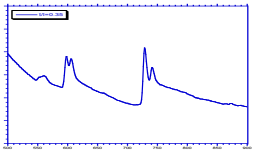

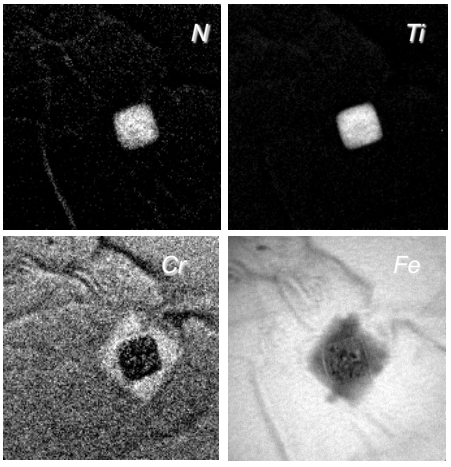

Zaluzec, Blackford - 2011

58

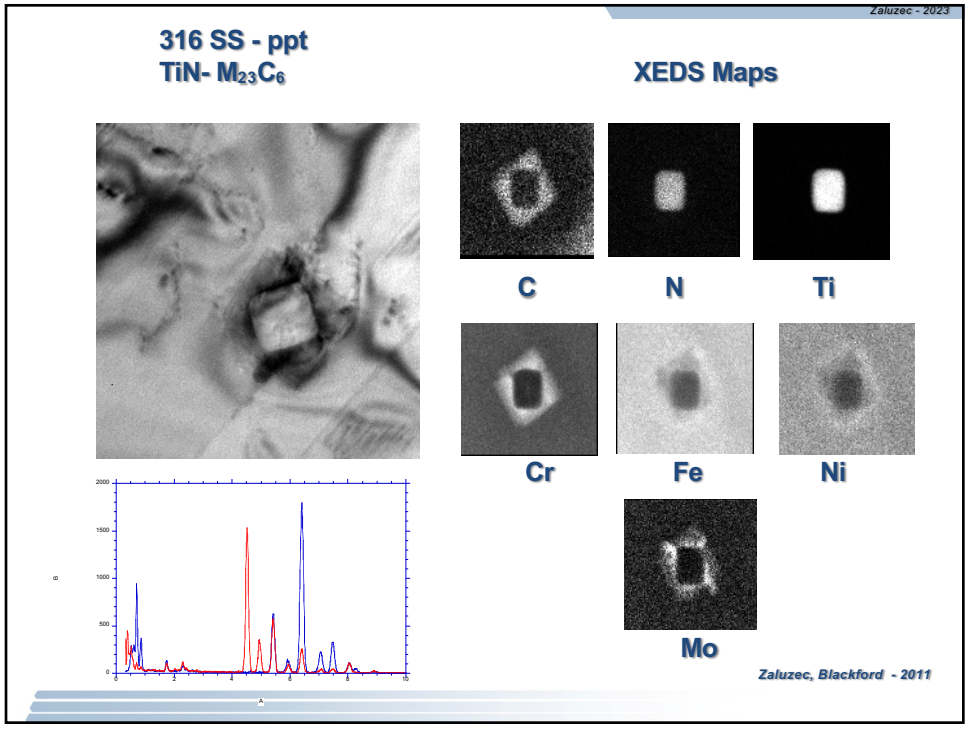
Zaluzec - 2023
316 SS - ppt
TiN- $M_{23}C_6$
XEDS Maps
C
N
Ti
Cr
Fe
Ni
Mo
Zaluzec, Blackford - 2011

59

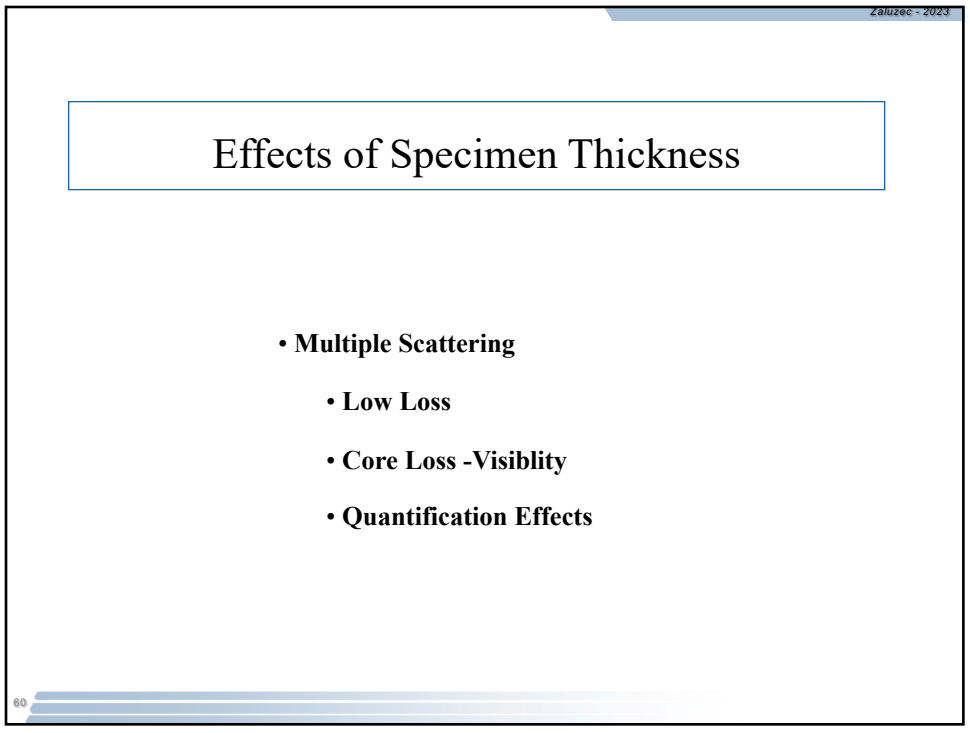
Zaluzec - 2023
Effects of Specimen Thickness
• Multiple Scattering
• Low Loss
• Core Loss -Visiblity
• Quantification Effects
60

60

Problems In EELS Quantification
Multiple Scattering

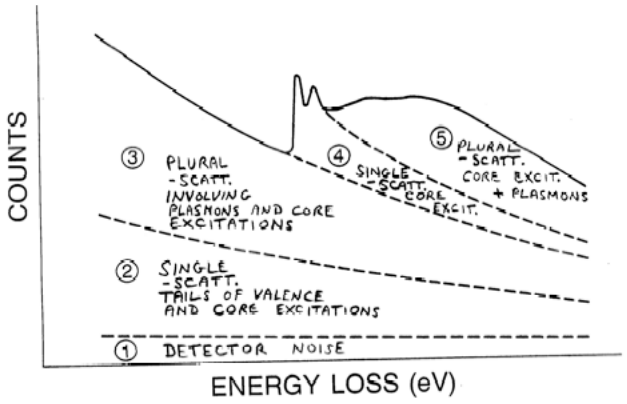

Leapman, 1991

61

- *To measure the thickness of compare the intensity of the zero loss (I_0) to the total integrated intensity in the spectrum (I_T).*
- *This ratio is directly proportional to the local thickness of the specimen.*

$$t / \lambda = \ln (I_T / I_0)$$

λ = *mean free path*

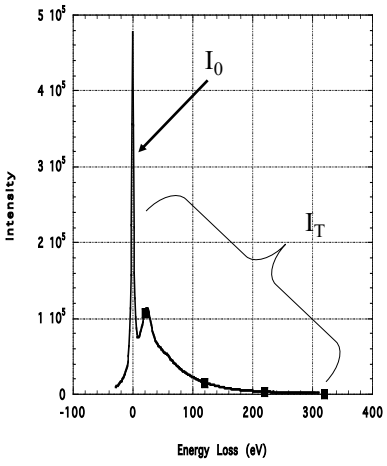

62

Zaluzec - 2023

Inelastic MFP:

$\lambda = 106\ F\ (E_0/E_m)/\ln(2\beta\ E_0/E_m)$

λ in nm,
β in mrad,
E_0 in keV
E_m in eV

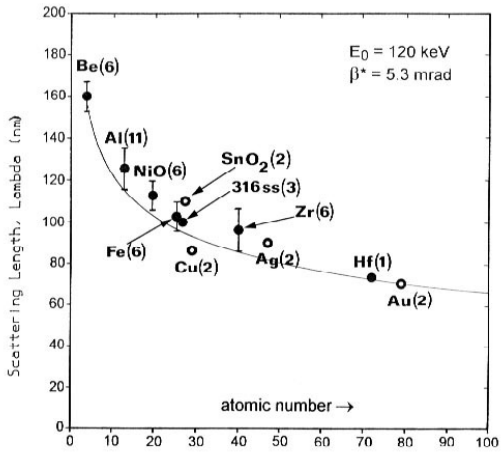

$E_m = 7.6Z^{0.36}$
$F = (1+E_0/1022\text{keV})/(1+E_0/511\text{keV})^2$

(Malis et al., JEMT 1988)

63

Zaluzec - 2023

Variation in EELS Edge P/B with Thickness

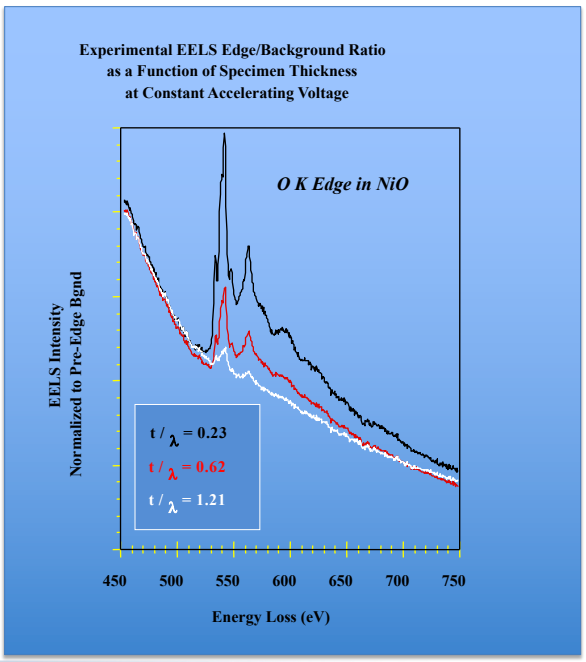

64

64

Variation in EELS Edge P/B with kV

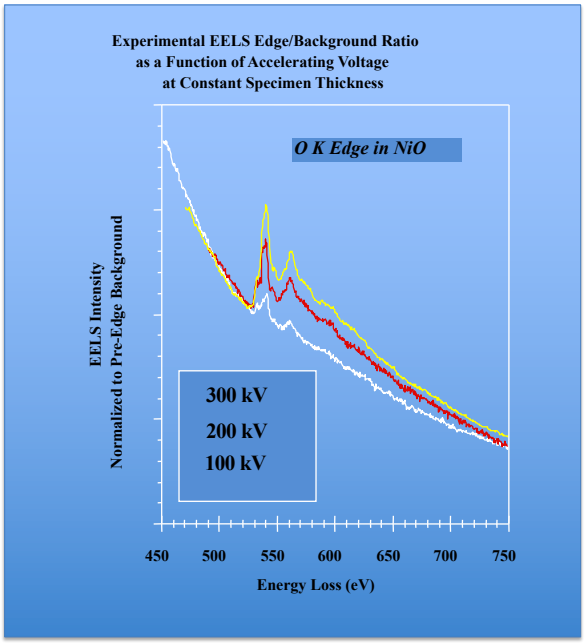

65

Specimen Thickness Effects on EELS

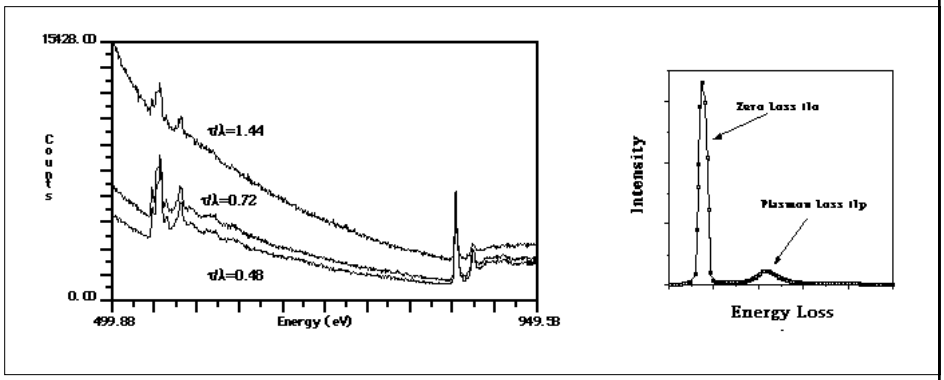

$$\frac{I_P}{I_o} = \frac{t}{\lambda} \leq 0.1$$

$$\ln\left(\frac{I_T}{I_o}\right) = \frac{t}{\lambda} \leq 1.0$$

66

Deconvolution of Multiple Scattering using Leapman/Swyt Method

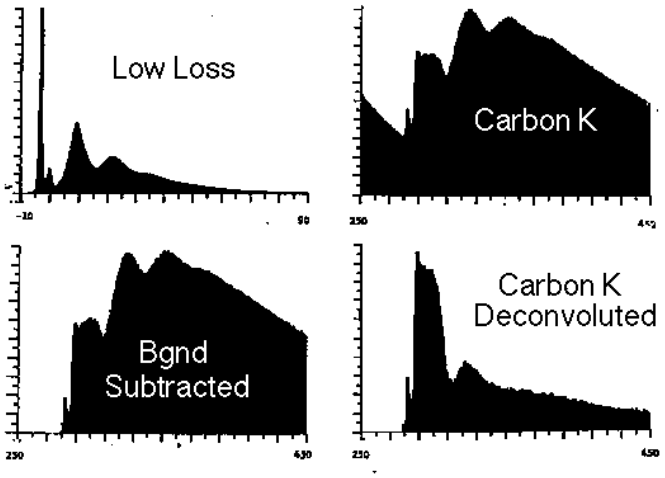

$MS = SS * LL$ $\qquad SS = \mathcal{F}^{-1}\left\{\frac{\mathcal{F}(MS)}{\mathcal{F}(LL)}\right\}$

$\mathcal{F}$ = *Fourier Transform* $\qquad \mathcal{F}^{-1}$ = *Inverse Fourier Transform*

67

67

Does Deconvolution Help Quantification?

$$\frac{I_A}{I_B} = \frac{\sigma_A N_A}{\sigma_B N_B}$$

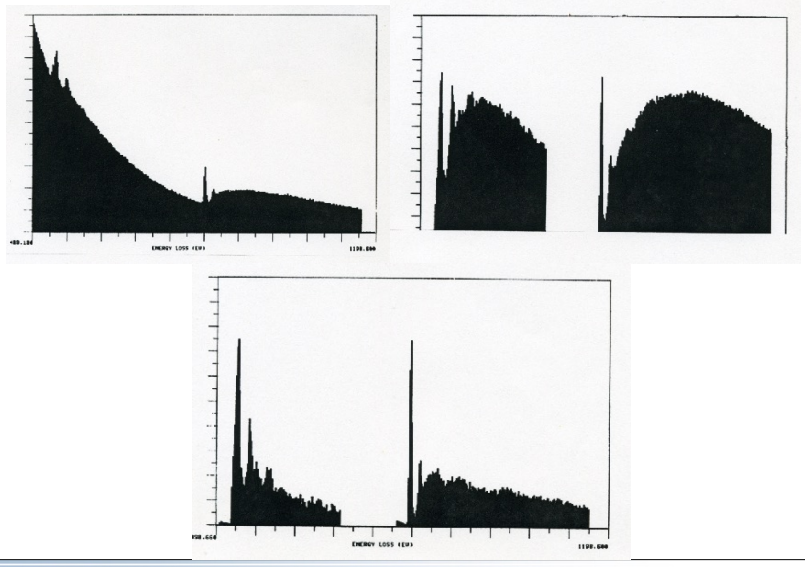

68

68

Does Deconvolution Help Quantification?

$$\frac{I_A}{I_B} = \frac{\sigma_A N_A}{\sigma_B N_B}$$

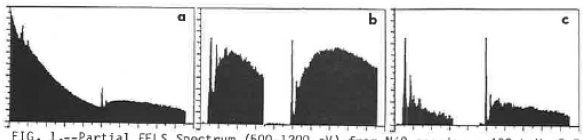

FIG. 1.--Partial EELS Spectrum (500-1200 eV) from NiO specimen: 100 keV, 5.7 mr scattering angle, a) unprocessed data b) background stripped, c) deconvoluted.

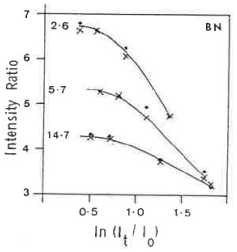

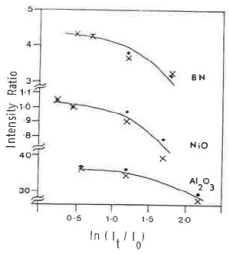

This defines a "Thin Film Approximation" for EELS i.e. $\frac{t}{\lambda} < 1.0$

69

69

Contamination Effects on EELS

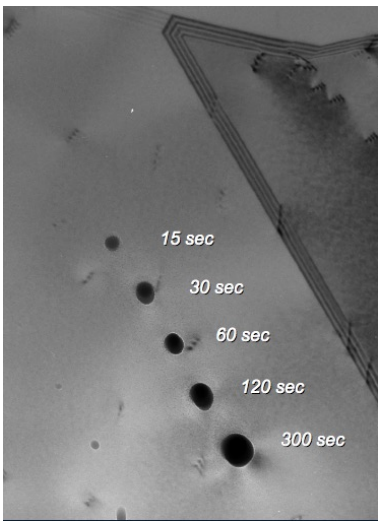

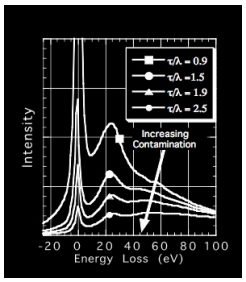

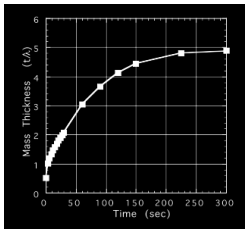

70

70

Spectral Imaging
Slice-by-Slice vs Point-by-Point

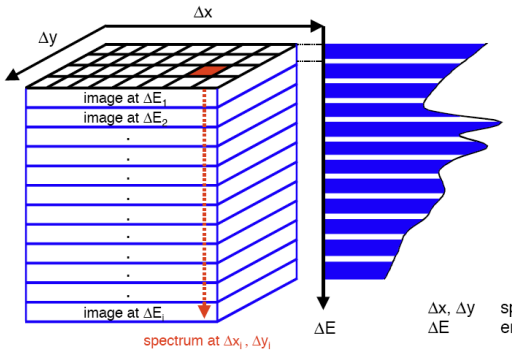

The technique of building up a more or less complete data cube is termed **Spectrum Imaging**

Δx, Δy spatial dimensions
ΔE energy-loss dimension

EFTEM Spectrum Imaging:
- Energy filtered broad beam technique
- fills data cube one image plane at a time
- less time

STEM Spectrum Imaging:
- Focused probe method
- fills data cube one spectrum at a time
- less dose

71

Elemental Mapping

Determine and subtract edge background using two pre-edge images to obtain the true edge signal

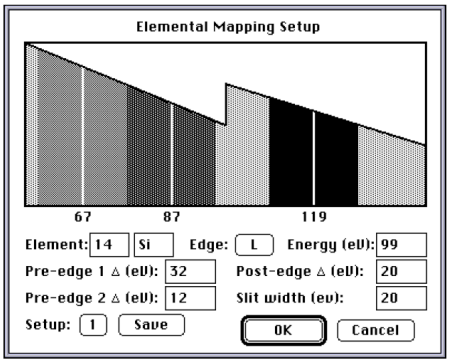

- Minimum of two background windows are necessary
- Map intensity is directly proportional to projected concentration
- Map-intensity can be related to absolute concentration if thickness and elemental cross-sections are known

Gatan Digital Micrograph

72

Elemental Mapping

6 layer metallization
test structure

recorded on a CM200, LaB6
with a GIF2002 (2K CCD)

field of view: 12 μm
number of pixels: 4.2 x 10^6

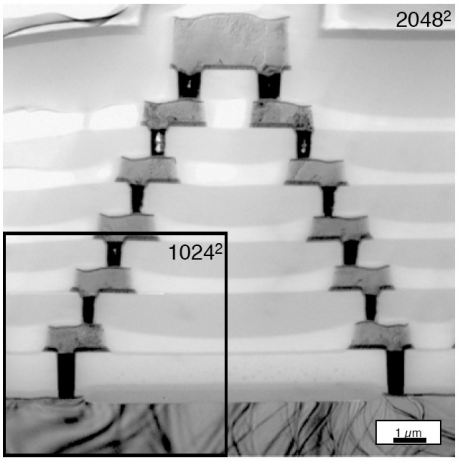

Gerald Kothleitner

73

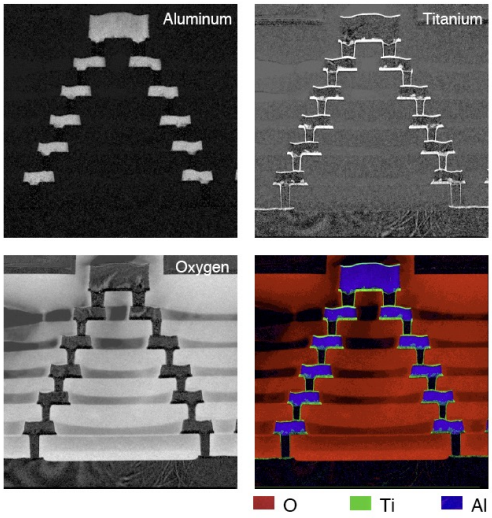

3 images each around:

O K edge: @ 532 eV
Ti L_{23} edge: @ 455 eV
Al K edge: @ 1560 eV

Color overlays,RGBimages:

- assign a color to each elemental map: O red, Ti green and Al blue

- superimpose three color layers to form RGB composite

Gerald Kothleitner

74

Leapman et al. (2003)

EFTEM elemental maps of mouse pancreatic Islet cells

Shows sulfur-rich insulin granules in β cells

Nitrogen
Phosphorus
Sulfur

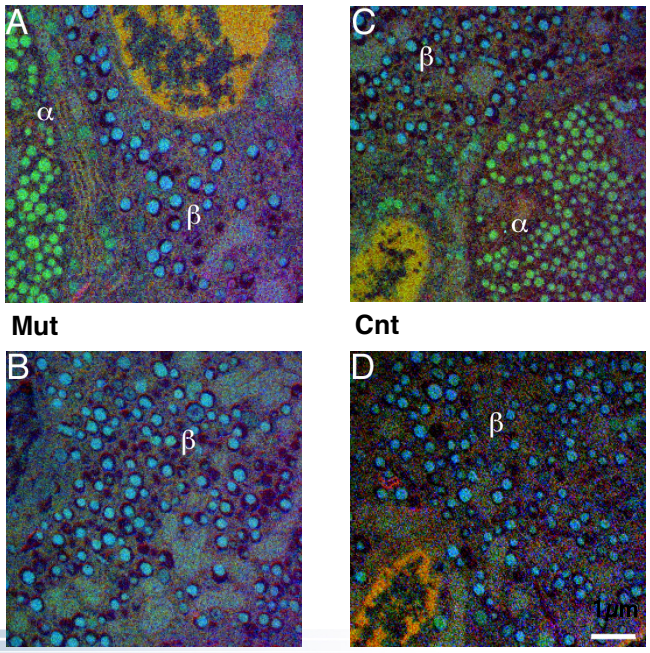

75

Adams *et al.*
Cell Chemical Biology
23 (2016 1417-1427

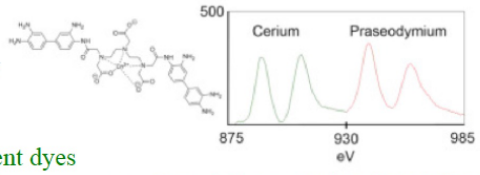

Equivalent of fluorescent dyes in optical microscopy but using lanthanides (Ce, Pr) and EFTEM imaging.

Cell endosome showing → surface protein (Ce, green) and short amino-acid chains (Pr, red) transported from the extracelluar environment.

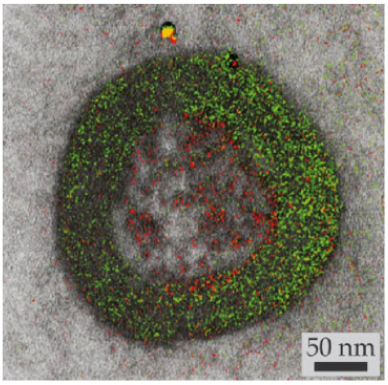

76

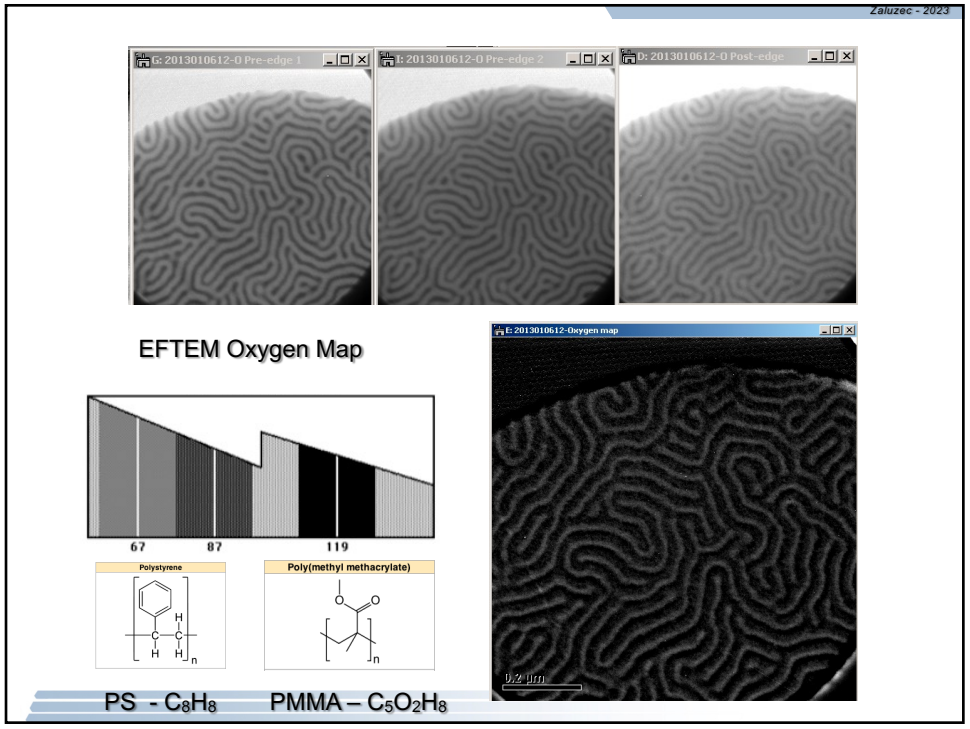
Zaluzec - 2023
D: 2013010612-O Pre-edge 1
I: 2013010612-O Pre-edge 2
D: 2013010612-O Post-edge
EFTEM Oxygen Map
E: 2013010612-Oxygen map
67
87
119
Polystyrene
Poly(methyl methacrylate)
0.2 µm
PS - C8H8
PMMA – C5O2H8

77

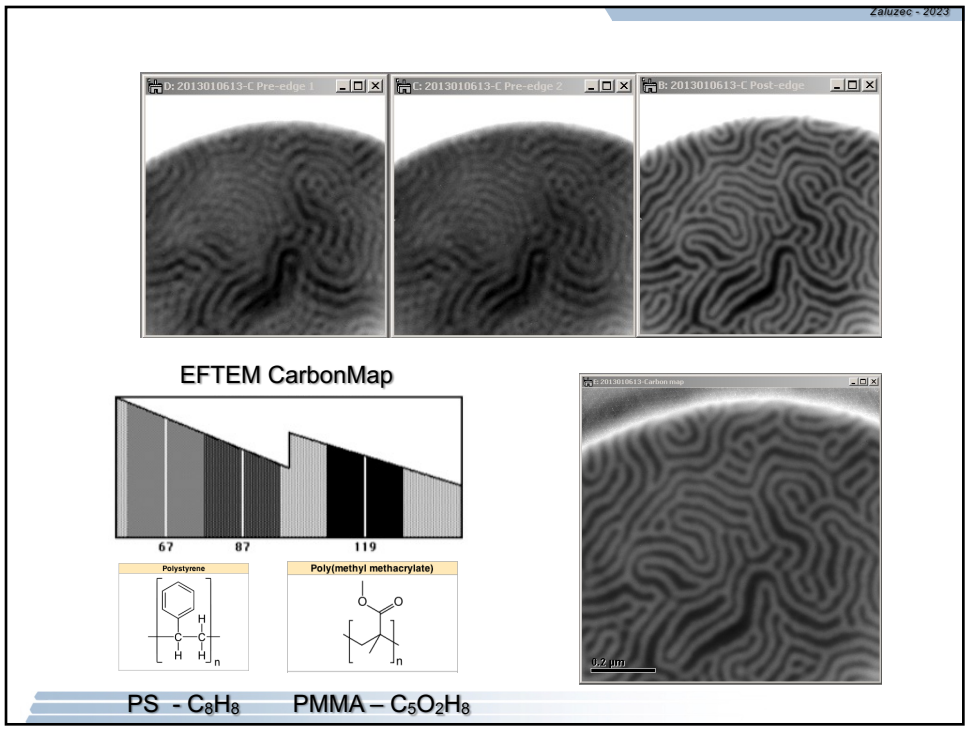
Zaluzec - 2023
D: 2013010613-C Pre-edge 1
C: 2013010613-C Pre-edge 2
D: 2013010613-C Post-edge
EFTEM CarbonMap
E: 2013010613-Carbon map
67
87
119
Polystyrene
Poly(methyl methacrylate)
0.2 µm
PS - C8H8
PMMA – C5O2H8

78

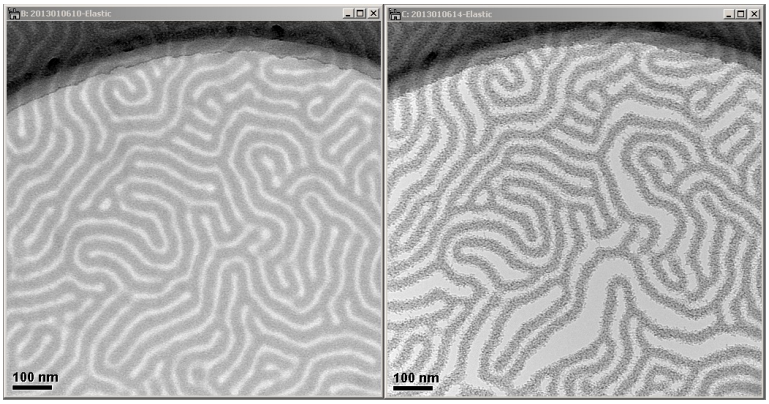

79

Steps in Quantitative (Elemental) Analysis

Select the operating mode: Is it appropriate?
- CTEM, STEM.....
- Image Coupled, Diffraction Coupled

Obtain a typical spectrum

Optimize the experimental conditions
- Accelerating Voltage (maximum consistent with your specimen)
- Chooze the best Edges to analyze (K, L, M,....)
- Optimize β for the weakest edges ($\theta_E = \delta E/2E_o$)
- Optimize α to minimize problems ($\alpha < \beta/2$)
- Optimize the Acquisition Mode
  - Normal - High Concentrations
  - Difference - Low Concentrations
- Optimize the Data Acquisition
  - Select Energy Resolution and Range
  - DQE & Statistics

Process the Data to Extract Intensities
- Normal
- Difference
- Reference Spectra

Check the relative specimen thickness ($t/\lambda < 1$□

Calculate the compositions
- Absolute # of atoms
- Relative # of atoms
- Standards/Standardless?

ReCheck for Artifacts/Problems
- Diffraction
- Orientation/Channeling
- Unidentified Edges
- Spectral Overlaps
- Radiation Damage

80

80

Linear Dichroism and Core Loss Electron Spectrosopy

Linear dichroism:

The linear polarization of the incident electrons parallel to the direction of momentum transfer. This polarization can be used sense the anisotropy of the valence states involved in the core excitation process. It can detect the number or changes in the number of the valence holes in different directions of the atomic volume.

In many cases, the anisotropy of the charge in the atomic volume is caused by crystal-field interaction and is due to an anisotropy in the bonding.

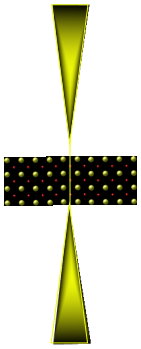

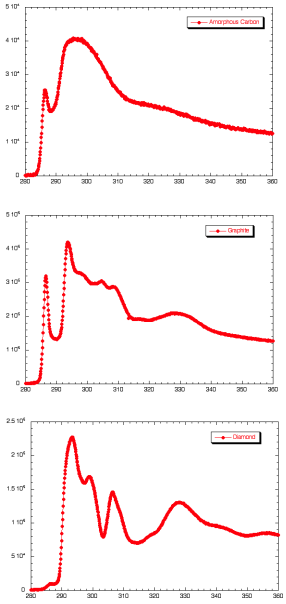

81

A Conventional EELS experiment in the TEM

Beam Convergence
2-10+ mR

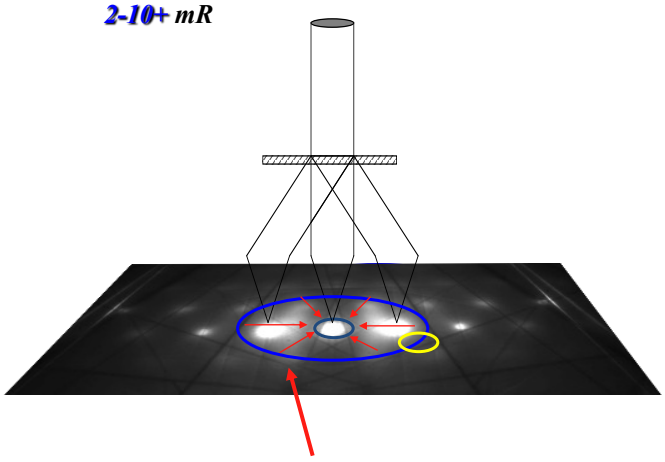

Angular Resolution typically 2-10 mR

82

Momentum Resolved EELS (MREELS) in Core Loss Spectroscopy derives its information from transitions from initial to final states

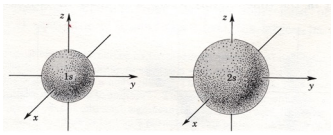

1s and 2s orbitals.

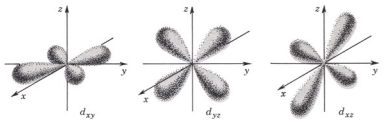

The five d orbitals.

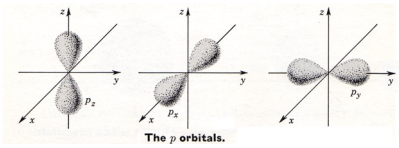

The p orbitals.

K shell p-> s L shell p->s and p->d

83

Energy Loss Disperson Surface

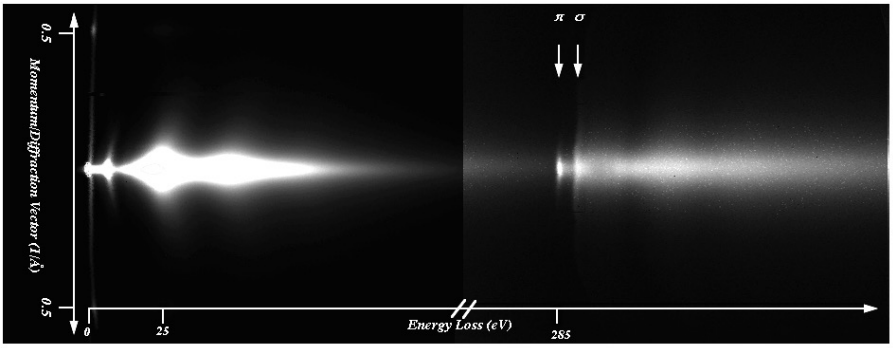

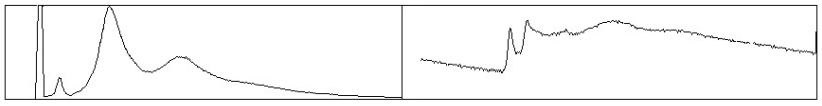

84

Core Loss Dispersion Surface

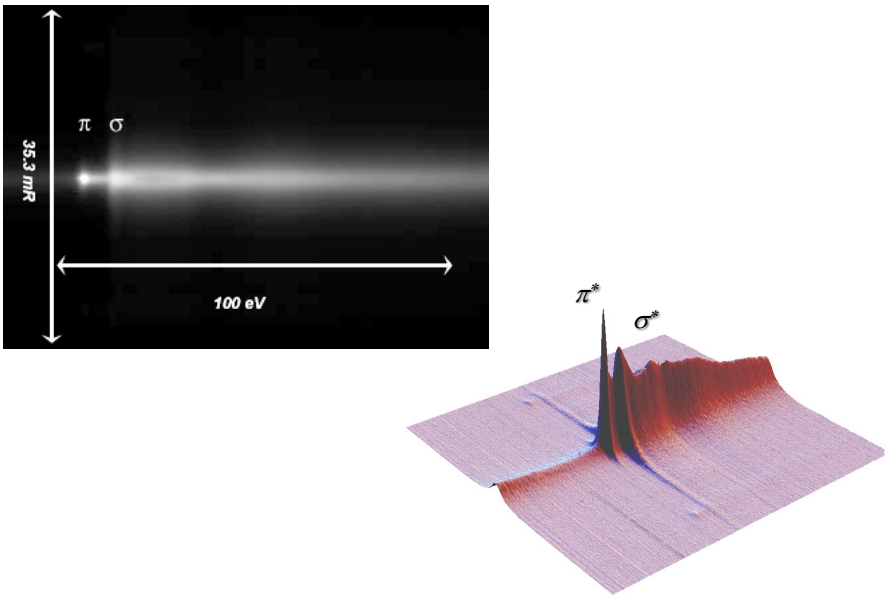

85

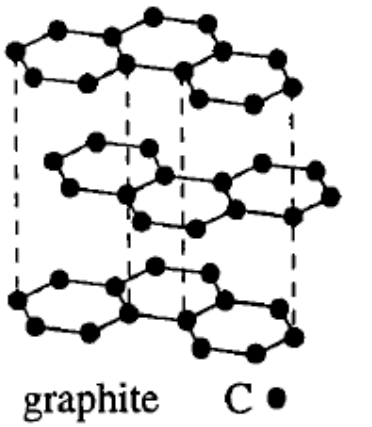

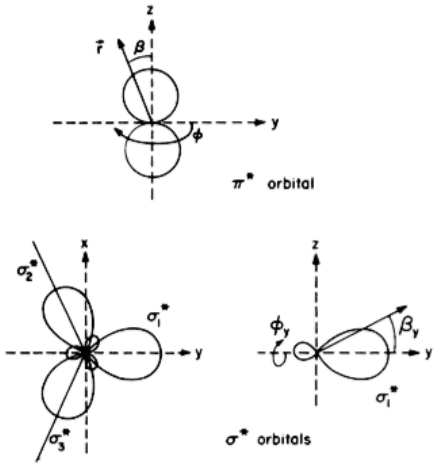

86

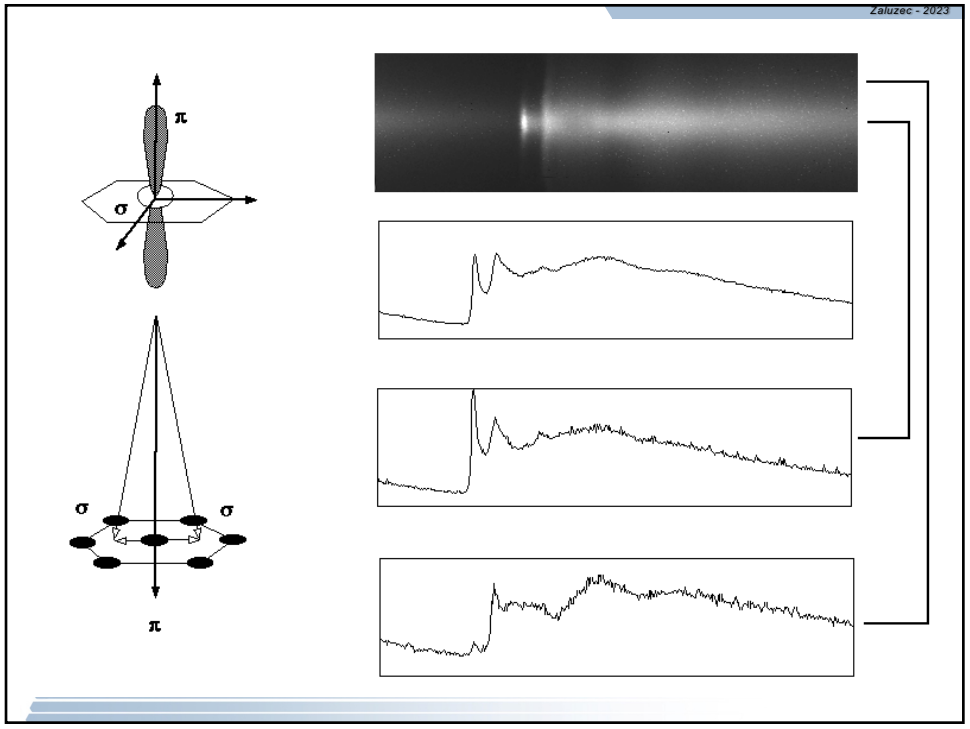

87

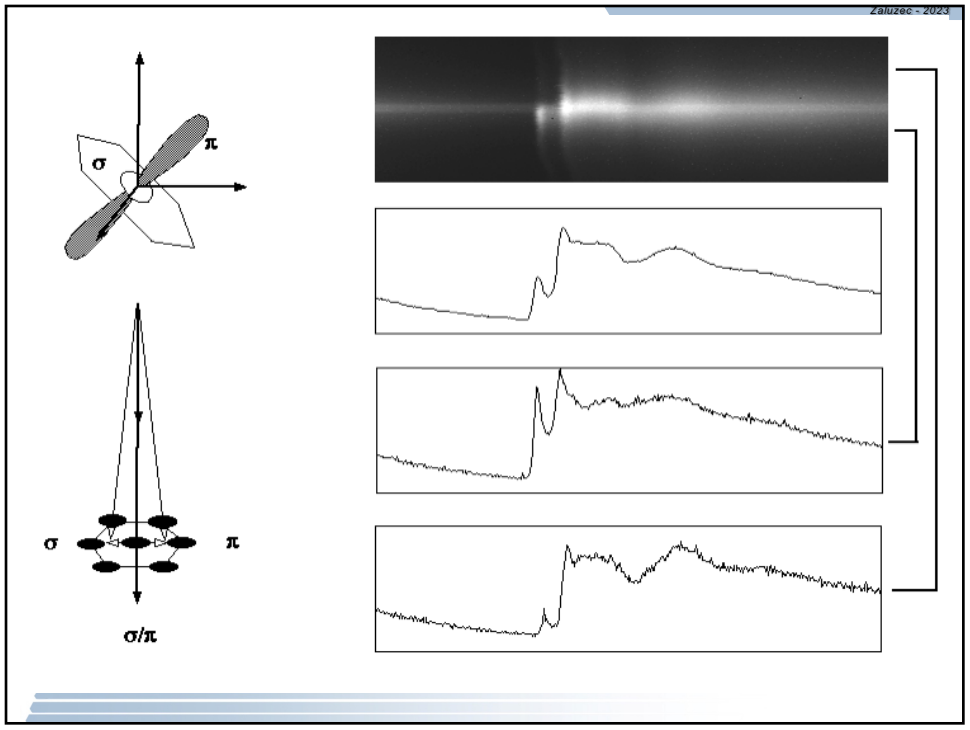

88

A Conventional EELS experiment in the TEM

Beam Convergence
2-10+ mR

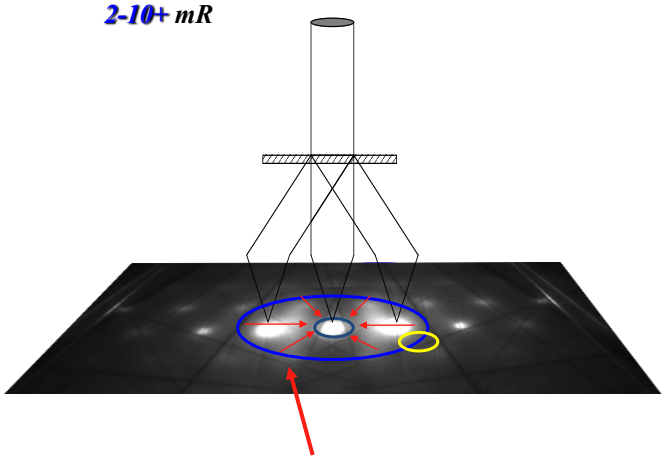

Angular Resolution typically 2-10 mR

89

Variation of Amorphous Carbon NES with Collection Angle (β)

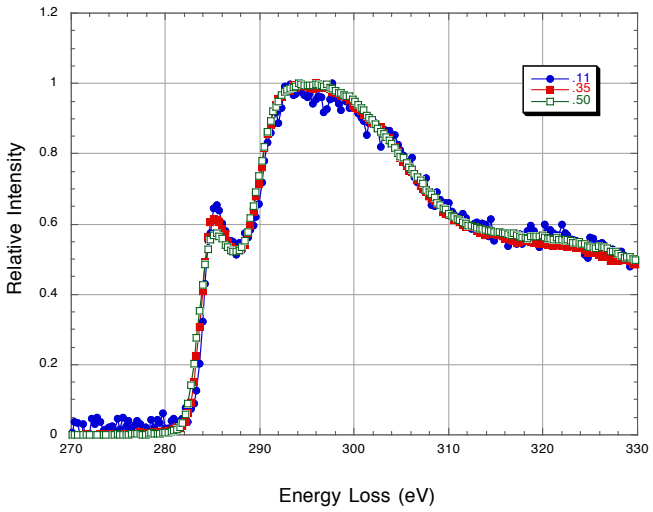

In some systems/conditions the difference is subtle
But …. this also depends upon what your looking for.

90

Variation of Graphite NES with Collection Angle (β)

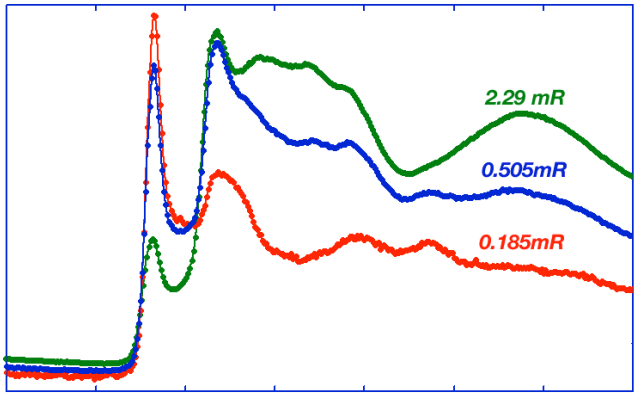

For Anisotropic Materials there can be large variations in the relative intensities of spectral features as a function of Angle (Momentum)

91

Variation of C_K (π^* σ^*) in Graphite with Scattering Angle

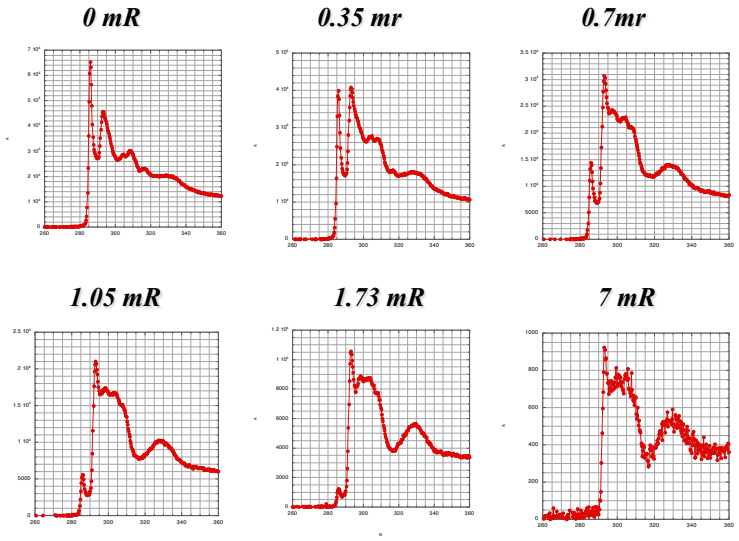

$\alpha_{1/2} \sim 0.025$ mR $\beta_{1/2} \sim 0.1$ mR $\theta_E \sim 1.15$ mR

92

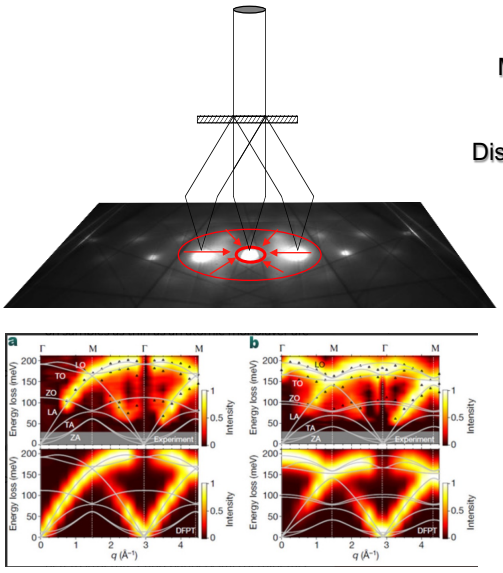

Momentum Resolved
HR EELS for
Phonon
Dispersion Measurements

Graphite

Hex - BN

Kazu Suenaga, AIST, Osaka, Japan

93

Additional Topics

Low Loss Spectroscopy
- Plasmon Losses Studies
- Dielectric Properties

Core Loss Spectroscopy
- Near Edge Structure
- Extended Fine Structure

Radiation Damage

94

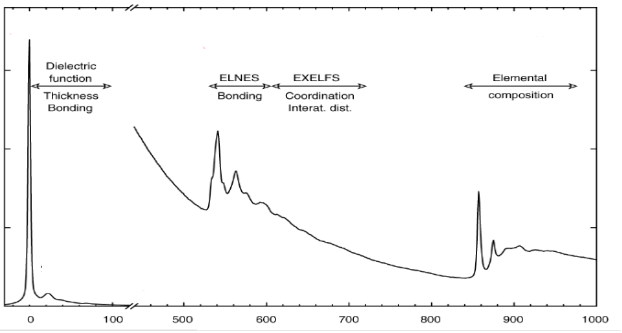

Low Loss Regime

Optical, Dielectric, Electronic, Magnetic Properties

Core Loss Regime

Composition, Bonding, Electronic, Magnetic , Structural Properties

Structure in EEL Spectra is a manifestation of:
Bonding (Chemistry/Physics) and/or Crystallography (Structure)

95

95

EELS Measurements of Valence Electron Densities

$$\text{Plasmon Energy} = E_p = \hbar\omega_p = \sqrt{\eta \frac{\hbar^2 e^2}{m \varepsilon_0}}$$

e is the elctron charge,
m its mass,
ε_0 the vacuum dielectric constant,
$\hbar$ = Planck's constant/2π
η the valence electron density

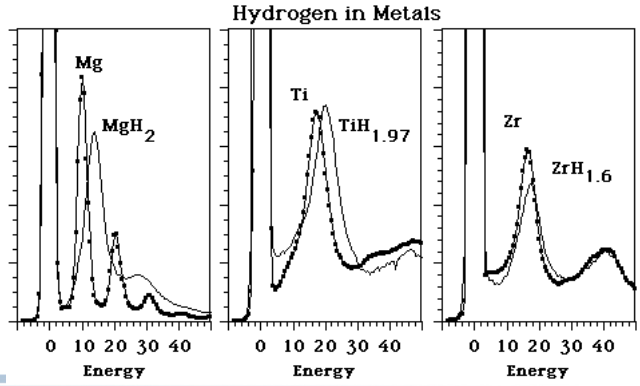

96

96

Table 2 Experimental and Calculated Plasmon Shifts in Selected Metal-Hydrogen Systems

Material	Expt. E_p (eV)	Calculated FEM	ΔE_p/H/M Expt.	ΔE_p/H/M FEM Calc.
Group II				
Mg	10.0 ± 0.5	10.90	2.1± 0.7	1.24
MgH_2	14.2± 0.5	13.38		
Group III				
Sc	14 + 2 eV	12.87	1.6± 0.7	1.50
ScH_2	17.2 ± 0.5	15.87		
Y	12.5 ± 0.2	11.19	1.4 ± 0.7	1.41
YH_2	15.3 ± 0.5	14.0		
Group IV				
Ti	17.2 ± 0.5	17.69	1.4± 0.7	0.87
$TiH_{1.97}$	20.0 ± 0.5	19.4		
Zr	16.6± 0.5	15.37	0.9± 0.7	0.91
$ZrH_{1.6}$	18.1± 0.5	16.83		
Group V				
V	22.0 ± 0.5	22.29	0.0	0.3
$VH_{0.5}$	22.0 ± 0.5	22.44		
PseudoGroup VI				
FeTi	22.0 ± 0.5	25.04/21.9*	0.0	-0.84/-0.3*
FeTiH(β)	22.0 ± 0.5	24.65/21.8*		
$FeTiH_2$(γ)	22.0 ± 0.5	24.15/21.5*		

* Calculated using modified FEM with $m_s=m_e$ and $m_d=1.9\ m_e$

97

$$E_p = \hbar\omega_p = \sqrt{\frac{n e^2}{\varepsilon_0}\left(\frac{\eta_s}{m_s}+\frac{\eta_d}{m_d}\right)}$$

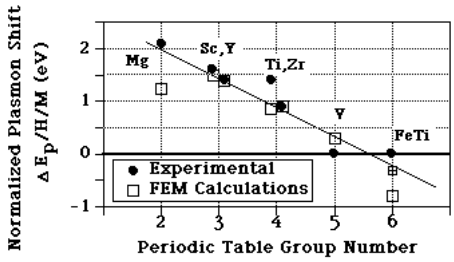

98

98

Information in Core-Loss Profiles

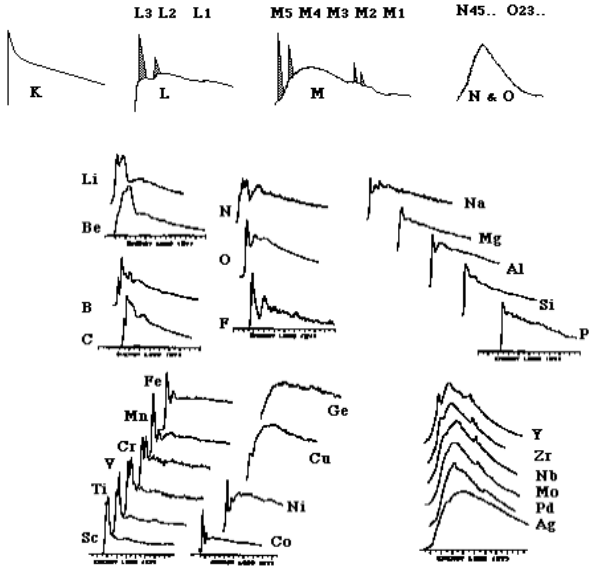

99

Additional EELS Information

Excitation of core levels by the transmitted electron beam can be used to measure the elemental composition of the solid, Near Edge Structure (NES) and EXtended Energy Loss Fine Structure (EXELFS) can be used to elucidate the density of states above the Fermi level and nearest neighbor configurations.

Oxygen K Shell in NiO

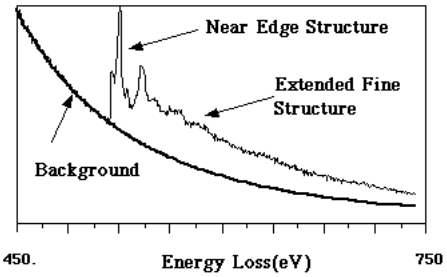

100

ELNES

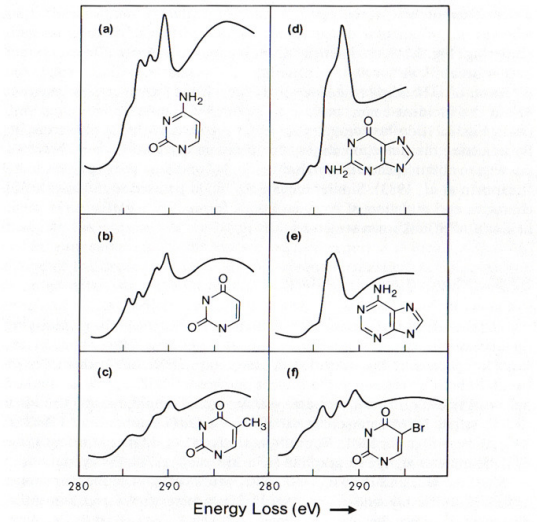

Figure 5.25. Carbon *K*-edge fine structure measured from thin films of (a) cytosine, (b) uracil, (c) thymine, (d) guanine, (e) adenine, and (f) bromothymine. Data from Isaacson (1972b) and Johnson (1972).

101

Copper L-shell Core Loss Spectroscopy in Metallic, Oxide and High Tc Superconductor Phases

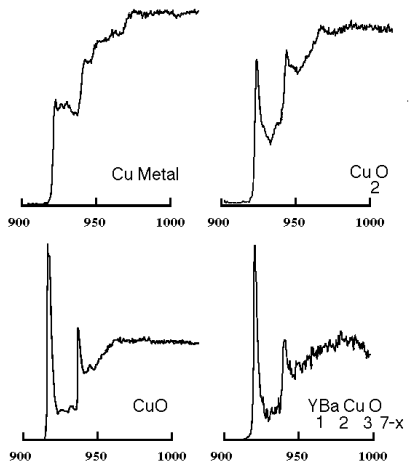

102

Fingerprinting of different oxidation states by comparing the fine-structure of the experimental core-loss peak with that of reference structures

High resolution EELS of Cu-V oxides: Application to batteries materials

Comparison between the V-$L_{2,3}$ spectra of the $Cu_{1.1}V_4O_{11}$ and the reference vanadium oxides. Comparison with reference spectra indicates that the vanadium is pentavalent.

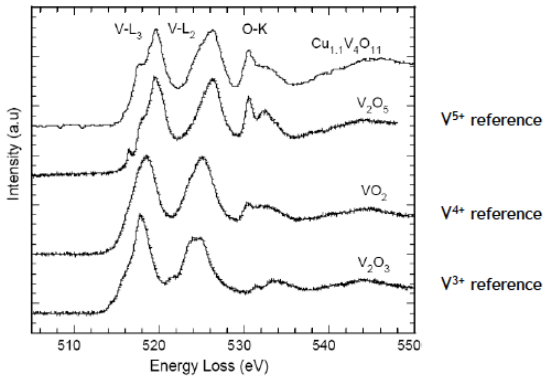

Laffont et al. Micron 37 (2006) 459, monochromized Tecnai 200ST (Delft)

103

103

Optical Properties of Metallic Nanoparticles

- *Optical properties of nanophase materials can be probed by EM radiation via excitation of surface plasmon resonances (SPR'S).*
- *Surface Plasmon Resonances are collective excitations of valence/conduction electron*
- *Frequency/Width of the surface modes are dependent upon dielectric constants of the nanostructures size, shape and local environment*
- *Requires excellent energy resolution in EEL Spectroscopy Mode to accurately measure.*

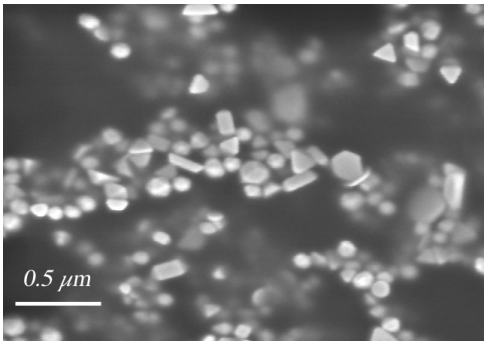

104

104

Optical Properties of Metal Nanoparticles
Influenced by Size, Shape, Local EM Fields & Dielectric Environment

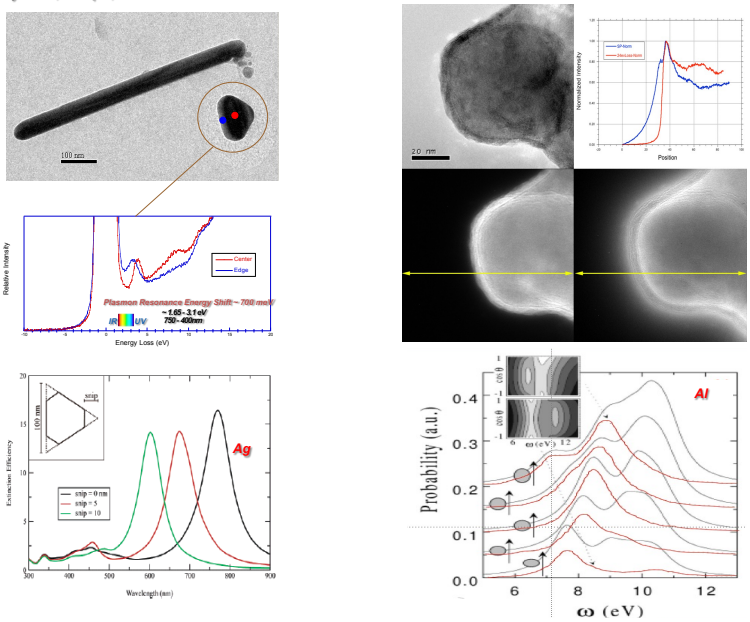

105

Electron Sources : Conventional XFEG vs CFEG
Compare Energy Resolution

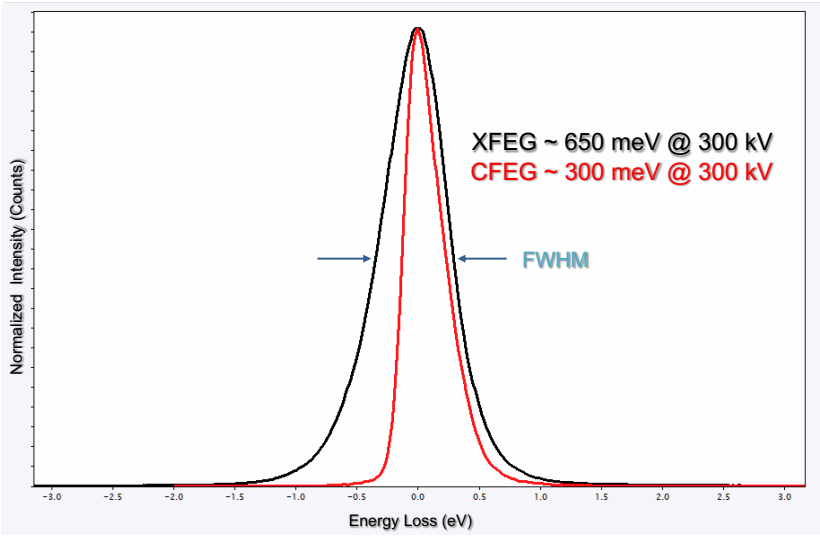

106

Zaluzec - 2023

Electron Source Energy Spread Comparisons
CFEG vs PicoProbe MonoChromated XFEG

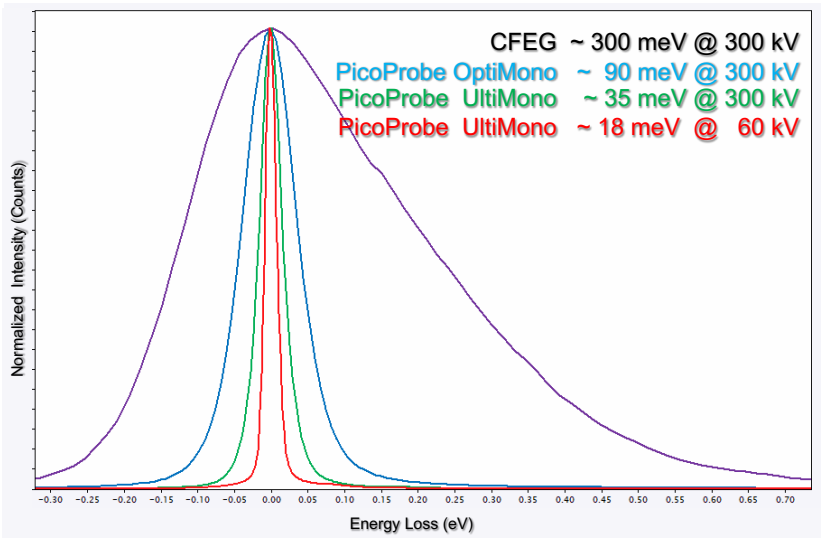

Pico Probe has the Highest Resolution Electron Energy Loss Spectrometry in the Midwest

but there is better i.e. Nion Ultra-Hermes DSTEM < 5 meV

107

Zaluzec - 2023

Tunable XFEG MonoChromator Performance
Facilitates Metrologically Relevant Measurements

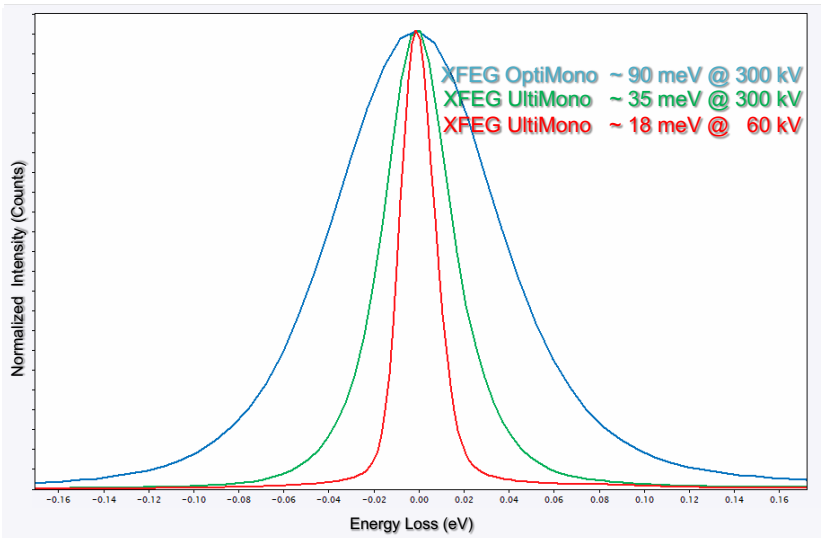

108

Zaluzec - 2023

HREELS is Essential for Low Loss / Vibrational Spectroscopy Studies

High Resolution UV/IR/Vibrational Low Loss Spectroscopy
at < 20 meV Resolution

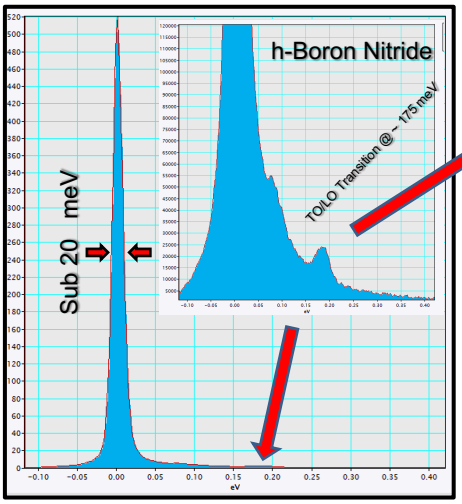

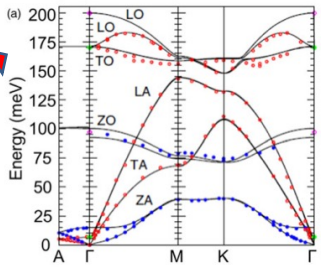

h-BN Phonon Dispersion Curves - Serrano etal
Phys Rev Lett 98, 095503.
2007

20230621 - BN @ 60 kV

109

Zaluzec - 2023

HREELS Vibrational Spectroscopy of Lithium Hydroxide

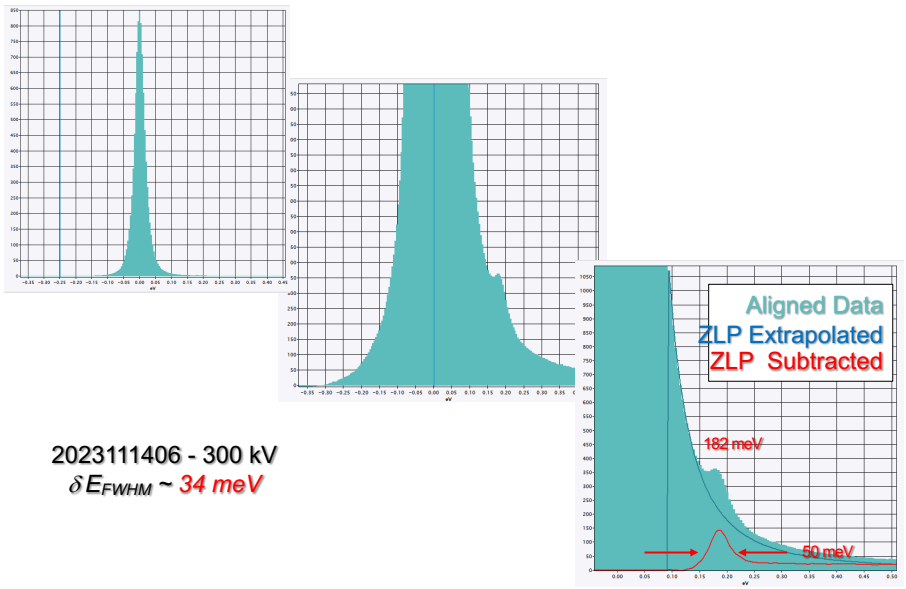

2023111406 - 300 kV
δE_{FWHM} ~ *34 meV*

ZLP Extrapolation and Subtraction

110

Plasmonics - Near Field / Surface Phenomena will enhance Signals

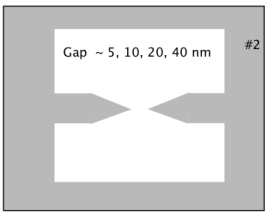

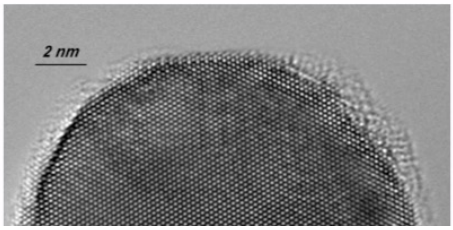

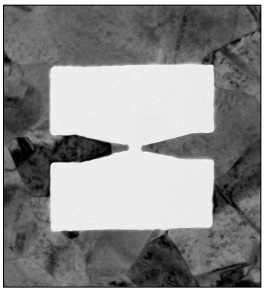

Au nano-antennae

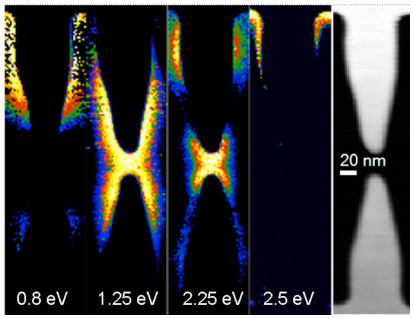

Monochromated HyperSpectral Imaging
1.65 - 3.1 eV <-> 750 - 400nm

Arenal etal. In press 2012

111

Optical Properties of Metal Nanoparticles

Influenced by Size, Shape, Local EM Fields & Dielectric Environment

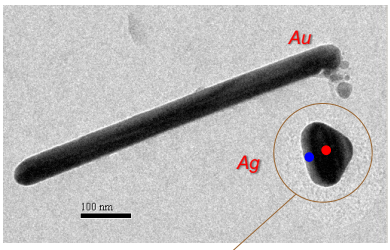

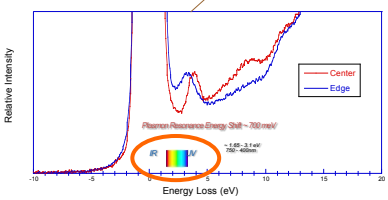

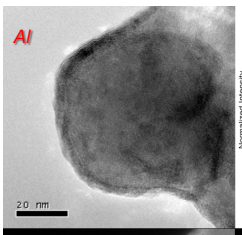

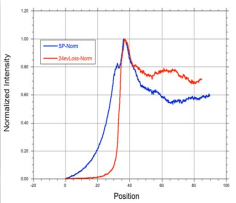

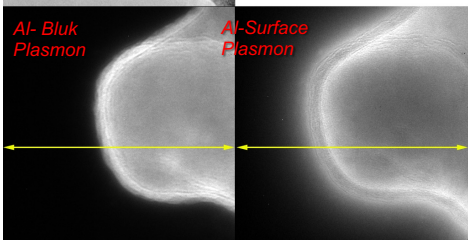

Plasmonic Spectroscopy is becoming increasingly useful
tool in our arsenal of characterization techniques =>> Applications to NP's and Adsorbates

112

Low energy-loss excitation modes within the dielectric model

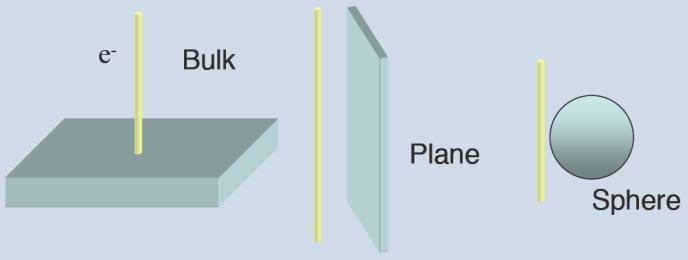

$P(\omega) \sim$	$\mathrm{Im}(-1/\varepsilon)$	$\mathrm{Im}((\varepsilon-1)/(1+\varepsilon))$	$\mathrm{Im}((\varepsilon-1)/(2+\varepsilon))$
Response function	Loss-function	Polarizability/surface	Polarizability (dipolar)
Within Drude model	ω_p	$\omega_s=\omega_p/\sqrt{2}$	$\omega_s=\omega_p/\sqrt{3}$

113

Photo-Induced Conversion of Ag nanospheres to Triangular Prisms Detecting Surface Plasmon Resonances

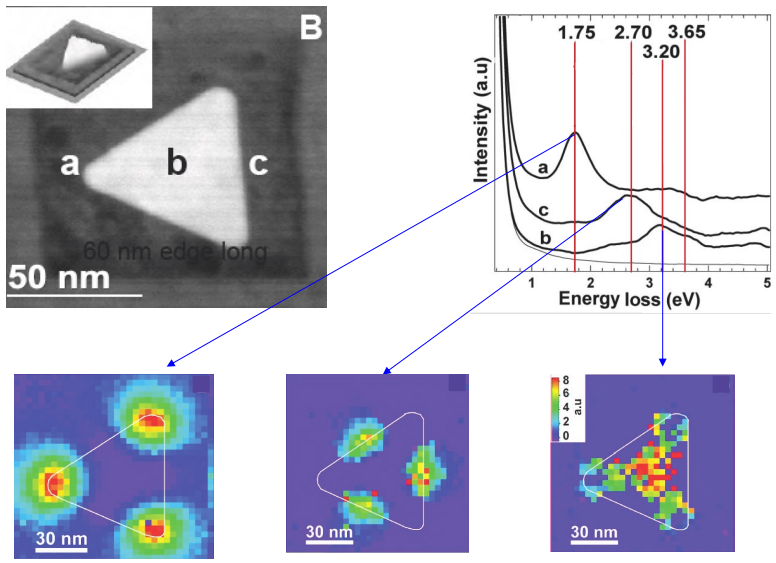

C. Colliex, L. Liz Marzan, I .Pastoriza-Santos - 2006

114

Excitation Modes Change with Shape!

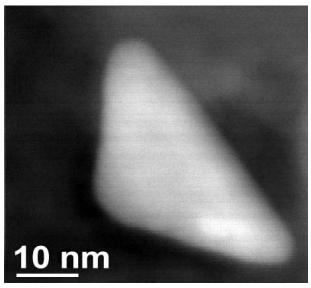

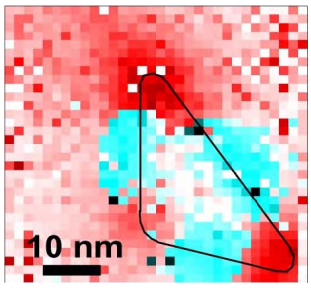

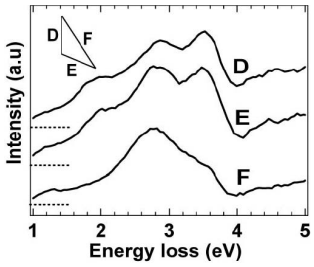

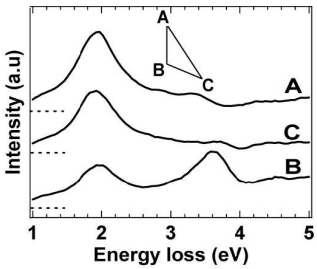

C. Colliex, L. Liz Marzan, I .Pastoriza-Santos - 2006

115

XEDS/EELS
Spectral Comparison

Intensity, Resolution & Signal/Background

Late 1970's – mid 1980' s
Si(Li) – XEDS / SEELS-PEELS

2000's ->
SDD/XEDS & Efilters/EELS

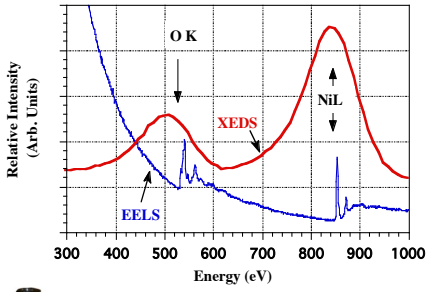

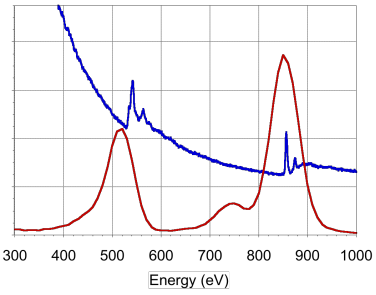

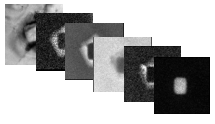

116

Test Specimen : Nickel Oxide - Compare the same Elemental Signals in XEDS and

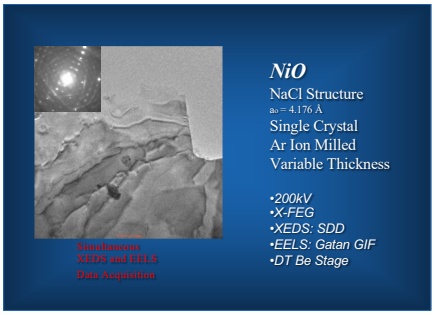

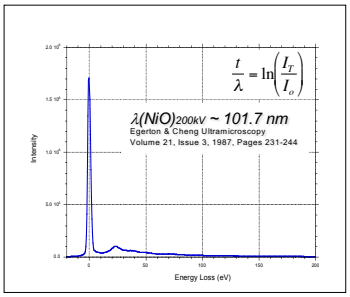

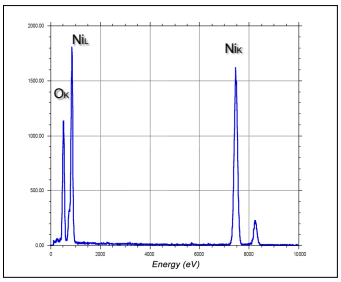

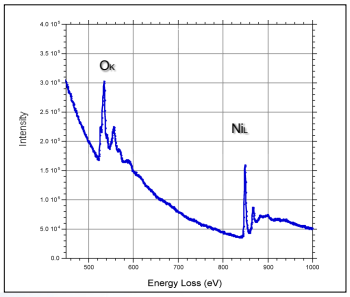

117

117

On the Performance of XEDS and EELS in the AEM: 25 Years Later

35

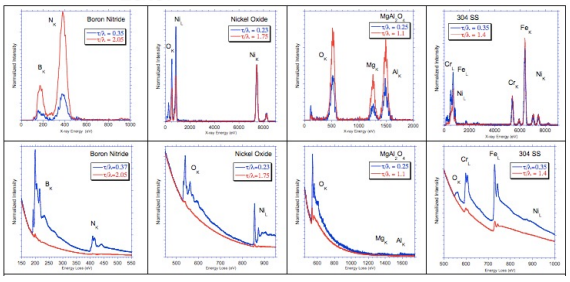

Ten Years have elapsed since the 2011 study and developments justify revisiting to see what has changed.

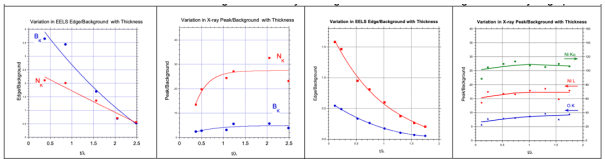

Fig. 2 Experimental measurements for BN vs t/λ, the integration windows for Edges, Peaks & Bg were identical for the respective data sets.

Fig. 3 Experimental measurements for NiO vs t/λ, the integration windows for Edges, Peaks & Bg were identical for the respective data sets.

On the Performance of XEDS and EELS in the AEM: 25 Years Later
H.L. Fraser , D.O. Klenov , Y.C. Wang , H. Cheng N. J. Zaluzec
Microsc. Microanal. 17 (Suppl 2), **2011**, 590-591 doi:10.1017/S1431927611003825

118

Zaluzec - 2023

Measurements - JEOL Mono NEOARM 200 F @ Chalmers University

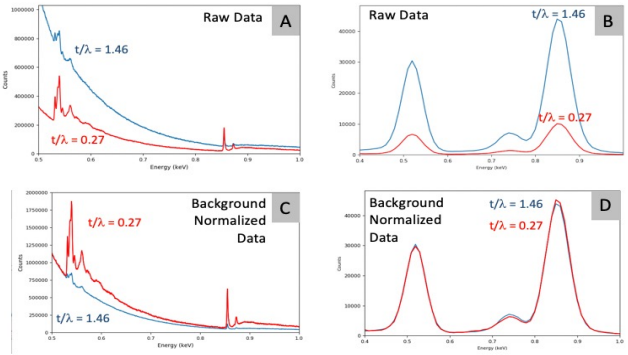

Comparison of EELS and XEDS showing the OK and NiL signals for two values of t/λ,
A & B are raw data, while C&D are normalized at the O_K background values.

Dual JEOL 100 mm^2 XEDS & Gatan Quantum HR.

119

Zaluzec - 2023

Measurements – NiO
JEOL Mono NEOARM 200 F @ Chalmers University
@ 60 kV & 200 kV

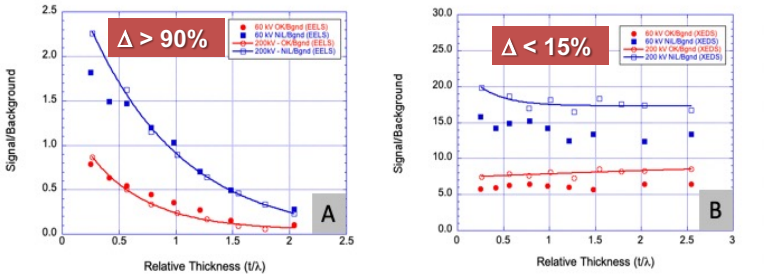

Experimental variation in the Signal/Background for EELS (A) and XEDS (B) measurements as a function of relative thickness at 60 and 200 kV. Solid lines are guides to the eye for 200 keV data. Note the relatively uniform I/B for XEDS vs EELS.

$$\frac{\Delta I}{I} \propto \mathrm{MDF} \propto \frac{k}{\sqrt{\frac{I^2}{(I+B)}}}$$ Both I & B vary with thickness

$$\mathrm{FoM}\ (\propto \mathrm{MDF})\ \frac{\Delta I_{t/\lambda}}{I_{t/\lambda}} \propto \frac{k}{\sqrt{\frac{I^2}{(I+B)*\left(\frac{t}{\lambda}\right)}}}$$ Thickness Normalization

120

Zaluzec - 2023

FoM Analysis – NiO
60 kV & 200 kV

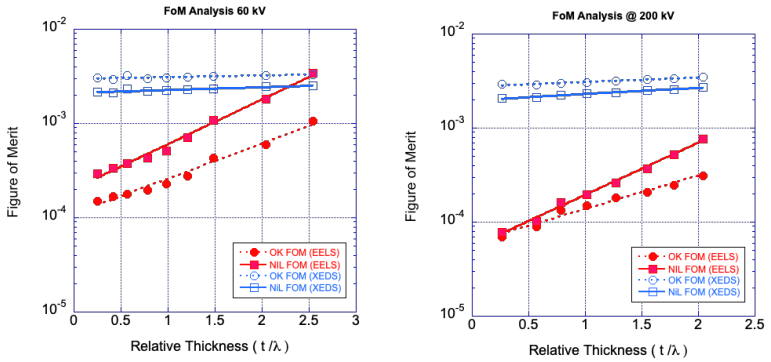

$$\text{FoM } (\propto \text{MDF}) \quad \frac{\Delta I_{t/\lambda}}{I_{t/\lambda}} \propto \frac{k}{\sqrt{\frac{I^2}{(1+B)*\left(\frac{t}{\lambda}\right)}}}$$

Note:

- *As E_o increases EELS improves due to the decreasing Bgnd due to reduction in multiple scattering*
- *Small difference vs E_o for XEDS because I/B does not change significantly*
- *A moderate improvement in XEDS detector efficiency will be significant as I will increase*

121

There are always Limiting Factors

Geometrical Broadening (all probes) $d_G \sim 2\alpha t$

α semiangle
t thickness

Beam Broadening (general scattering) $d_B \sim 625\frac{Z}{E_o}\left(\sqrt{\frac{\rho}{A}}\right)t^{3/2}$

d_B (cm)
t thickness(cm)
ρ density (gm/cm^3)
E_0 Accelerating Voltage (keV)
Z, A atomic number & wt

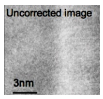

Chromatic Broadening (EFTEM) $d_C \sim FC_c\beta\frac{\Delta_S}{E_o}$

Cc Chromatic Ab Coeff (mm -> μm)
β Scattering semiangle (mR)
Δ_s Energy Window/Slit Width (eV)
E_0 Accelerating Voltage (keV)
F Factor 0.1 (low loss) -0.3 (high loss)

Inelastic Delocalization $d_L \sim 0.44\frac{\lambda}{\theta_E^{3/4}}$ $\theta_E = \frac{\Delta E}{2T_0}$ $T_0 = \gamma m_0 c^2$

λ Electron Wavelength
θ_E Mean Scattering angle
ΔE Energy Loss
T_o Electron Kinetic Energy

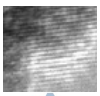

Image/Diffraction Delocalization $d_R = |\, C_5 \square^5 g^5 + C_3 \square^3 g^3 + \square \square f\, g \,|_{max}$

$C_3 = C_s$
g diffract. vector
Δf defocus

122

Table 2.1. Summary of the analytical uses of EELS

Property determined	Spectral region	Processing required	Uses/limitations
Sample thickness	Full spectrum or low loss region	Integration of intensities	Rapid measure of relative thickness; need Λ (inelastic) for absolute values.
Valence electron density	Low loss – plasmon peak position	Peak fitting if required	Phase Identification/ Effects of alloying
Surface/interface states	Low loss – surface plasmons	Need model of dielectric function based on geometry	Surface properties
Joint DOS	Low loss – energy loss function	Deconvolution/fitting of ZLP/Kramers Kronig analysis/sum rules	Band gaps/interband transitions/comparison with optical results
Elemental concentration/ elemental distributions (EFTEM)	High loss – ionization edge intensities	Background subtraction/ deconvolution/ integration/calculation of partial cross-sections	Good for light elements with edges in range 0–2.5 keV/ often high detection limits/limited to thin sample areas
Element specific local coordination and/or valency	High loss – ELNES	Deconvolution/ comparison with reference materials – fingerprinting/peak fitting	Need good energy resolution and determination of absolute energy loss
Element specific unoccupied DOS	High loss – ELNES	Deconvolution/modelling of electronic structure	Need good energy resolution/effect of the core hole
Element specific radial distribution function	High loss – EXELFS	Standard EXAFS data processing	Low SNR – requires good statistics and large edge separations
Anisotropic DOS	High loss – ELNES/ low loss	Deconvolution/modelling of electronic structure	Need small collection angles and well-defined specimen orientation
Site specific DOS	High loss – ELNES/ALCHEMI	Deconvolution/modelling of electronic structure	Need well-defined diffraction and collection conditions
Ground state electron momentum distribution at large momentum transfer	Compton profile	Standard Compton scattering data processing	Low SNR/diffraction conditions

123

124